NATIONAL ADVISORY COMMITTEE FOR AERONAUTICS

REPORT No. 652

AIR FLOW IN THE BOUNDARY LAYER OF AN ELLIPTIC CYLINDER

By G. B. SCHUBAUER

1939

For sale by the Superintendent of Documents, Washington, D. C. - - - - - - - - - - Price 10 cents
Subscription price, $3.00 per year

AERONAUTIC SYMBOLS

1. FUNDAMENTAL AND DERIVED UNITS

	Symbol	Metric		English	
		Unit	Abbreviation	Unit	Abbreviation
Length	l	meter	m	foot (or mile)	ft. (or mi.)
Time	t	second	s	second (or hour)	sec. (or hr.)
Force	F	weight of 1 kilogram	kg	weight of 1 pound	lb.
Power	P	horsepower (metric)		horsepower	hp.
Speed	V	kilometers per hour	k.p.h.	miles per hour	m.p.h.
		meters per second	m.p.s.	feet per second	f.p.s.

2. GENERAL SYMBOLS

W, Weight $=mg$

g, Standard acceleration of gravity $=9.80665$ m/s^2 or 32.1740 ft./sec.^{2}

m, Mass $=\frac{W}{g}$

I, Moment of inertia $=mk^2$. (Indicate axis of radius of gyration k by proper subscript.)

u, Coefficient of viscosity

ν, Kinematic viscosity

ρ, Density (mass per unit volume)

Standard density of dry air, 0.12497 kg-m^{-4}-s^2 at 15° C. and 760 mm; or 0.002378 lb.-ft.$^{-4}$ sec.^{2}

Specific weight of "standard" air, 1.2255 kg/m^3 or 0.07651 lb./cu. ft.

3. AERODYNAMIC SYMBOLS

S, Area

S_w, Area of wing

G, Gap

b, Span

c, Chord

$\frac{b^2}{S}$, Aspect ratio

V, True air speed

q, Dynamic pressure $=\frac{1}{2}\rho V^2$

L, Lift, absolute coefficient $C_L=\frac{L}{qS}$

D, Drag, absolute coefficient $C_D=\frac{D}{qS}$

D_0, Profile drag, absolute coefficient $C_{D_0}=\frac{D_0}{qS}$

D_i, Induced drag, absolute coefficient $C_{D_i}=\frac{D_i}{qS}$

D_p, Parasite drag, absolute coefficient $C_{D_p}=\frac{D_p}{qS}$

C, Cross-wind force, absolute coefficient $C_C=\frac{C}{qS}$

R, Resultant force

i_w, Angle of setting of wings (relative to thrust line)

i_s, Angle of stabilizer setting (relative to thrust line)

Q, Resultant moment

Ω, Resultant angular velocity

$\rho\frac{Vl}{\mu}$, Reynolds Number, where l is a linear dimension (e.g., for a model airfoil 3 in. chord, 100 m.p.h. normal pressure at 15° C., the corresponding number is 234,000; or for a model of 10 cm chord, 40 m.p.s., the corresponding number is 274,000)

C_p, Center-of-pressure coefficient (ratio of distance of c.p. from leading edge to chord length)

α, Angle of attack

ϵ, Angle of downwash

α_0, Angle of attack, infinite aspect ratio

α_i, Angle of attack, induced

α_a, Angle of attack, absolute (measured from zero-lift position)

γ, Flight-path angle

REPORT No. 652

AIR FLOW IN THE BOUNDARY LAYER OF AN ELLIPTIC CYLINDER

By G. B. SCHUBAUER

National Bureau of Standards

127090—39

NATIONAL ADVISORY COMMITTEE FOR AERONAUTICS

HEADQUARTERS, NAVY BUILDING, WASHINGTON, D. C.

LABORATORIES, LANGLEY FIELD, VA.

Created by act of Congress approved March 3, 1915, for the supervision and direction of the scientific study of the problems of flight (U. S. Code, Title 50, Sec. 151). Its membership was increased to 15 by act approved March 2, 1929. The members are appointed by the President, and serve as such without compensation.

TECHNICAL COMMITTEES

AERODYNAMICS
POWER PLANTS FOR AIRCRAFT
AIRCRAFT MATERIALS

AIRCRAFT STRUCTURES
AIRCRAFT ACCIDENTS
INVENTIONS AND DESIGNS

Coordination of Research Needs of Military and Civil Aviation

Preparation of Research Programs

Allocation of Problems

Prevention of Duplication

Consideration of Inventions

LANGLEY MEMORIAL AERONAUTICAL LABORATORY

LANGLEY FIELD, VA.

Unified conduct, for all agencies, of scientific research on the fundamental problems of flight.

OFFICE OF AERONAUTICAL INTELLIGENCE

WASHINGTON, D. C.

Collection, classification, compilation, and dissemination of scientific and technical information on aeronautics.

5-24-39

REPORT No. 652

AIR FLOW IN THE BOUNDARY LAYER OF AN ELLIPTIC CYLINDER

By G. B. Schubauer

SUMMARY

The boundary layer of an elliptic cylinder of major and minor axes 11.78 and 3.98 inches, respectively, was investigated in an air stream in which the turbulence could be varied. Conditions were arranged so that the flow was two-dimensional with the major axis of the ellipse parallel to the undisturbed stream. Speed distributions across the boundary layer were determined with a hot-wire anemometer at a number of positions about the surface for the lowest and highest intensities of turbulence, with the air speed in both cases sufficiently high to produce a turbulent boundary layer over the downstream part of the surface. The magnitude and the frequency of the speed fluctuations in the boundary layer were also measured by the use of the conventional type of hot-wire turbulence apparatus. Stream turbulence was found to affect both the nature of transition from laminar to turbulent flow in the layer and the position on the surface at which transition occurred.

Transition was then investigated in detail with stream turbulence of several different scales and intensities. It was found that the position of transition could be expressed as a function of the intensity divided by the fifth root of the scale.

INTRODUCTION

The present boundary-layer investigation was conducted on an elliptic cylinder of major and minor axes 11.78 and 3.98 inches, respectively, placed in the 4½-foot wind tunnel of the National Bureau of Standards with the major axis of the ellipse parallel to the wind. This same cylinder, similarly placed in the same tunnel, was used in earlier work (reference 1), in which the laminar boundary layer and the laminar separation were investigated at a low air speed. The present investigation was carried out for the purpose of supplementing the earlier work with information on the boundary layer under such conditions of air speed and turbulence that transition occurs and the layer is partly laminar and partly turbulent. The investigation comprised the measurement of mean speeds and speed fluctuations in various sections of the boundary layer and the location of the transition and the separation points. Special attention was given to the nature and the position of the transition and the manner in which they are affected by stream turbulence and Reynolds Number.

In the work reported in reference 1, the air speed was about 12 feet per second, and it was assumed that the boundary layer remained in the laminar condition until after separation because the separation point remained fixed and the pressure distribution about the cylinder was unaffected until an air speed of about 15 feet per second was reached. Above 15 feet per second the separation point began to shift toward the trailing edge and the pressure distribution began to change, indicating that transition was beginning either in the attached part of the layer or in the separated layer near enough to the cylinder to affect the flow. It was therefore assumed that a turbulent layer could be obtained over the rear part of the cylinder simply by increasing the speed. Accordingly, at the outset of the present work, the pressure distribution was determined at successively increasing speeds until a critical speed region, similar to that found with spheres, had been passed and the pressure distribution again attained a stationary value. The critical region ended in the neighborhood of 55 feet per second. Since the downstream part of the boundary layer was assumed to be turbulent above the critical region, a speed of 70 feet per second was chosen as a suitable working speed for the boundary-layer investigation.

Not until the speed profiles in the boundary layer had been determined at numerous points about the surface and studies of separation had been made, was it discovered that the actual flow conditions were more complicated than those originally assumed. There first occurred the separation of a layer having the general characteristics of a laminar layer; this separation was followed by a reattachment of the layer to the surface as a turbulent layer; and finally the separation of the turbulent layer occurred. In this part of the work, the stream turbulence was as low as could be attained in the tunnel.

Under such conditions the turbulent layer was too limited in extent for the type of investigation originally planned, and an effort was made to obtain a greater length of turbulent layer by increasing the turbulence of the air stream with a 1-inch square mesh screen placed 18 inches upstream from the leading edge of the cylinder. This increased turbulence was found to have a marked effect on the layer, in that a turbulent layer developed without the intervening separation. Since the layer was now more like that originally sought, the measurements were repeated.

When it was found from the measurements that the amount of stream turbulence had an important effect on transition from laminar to turbulent flow in the layer, the investigation was extended to include a detailed study of transition as a function of both the scale and the intensity of the turbulence.

The present investigation therefore covers:

1. Boundary-layer phenomena at low stream turbulence.

2. Boundary-layer phenomena at high stream turbulence.

3. The effect of intensity and scale of stream turbulence on transition at a fixed Reynolds Number.

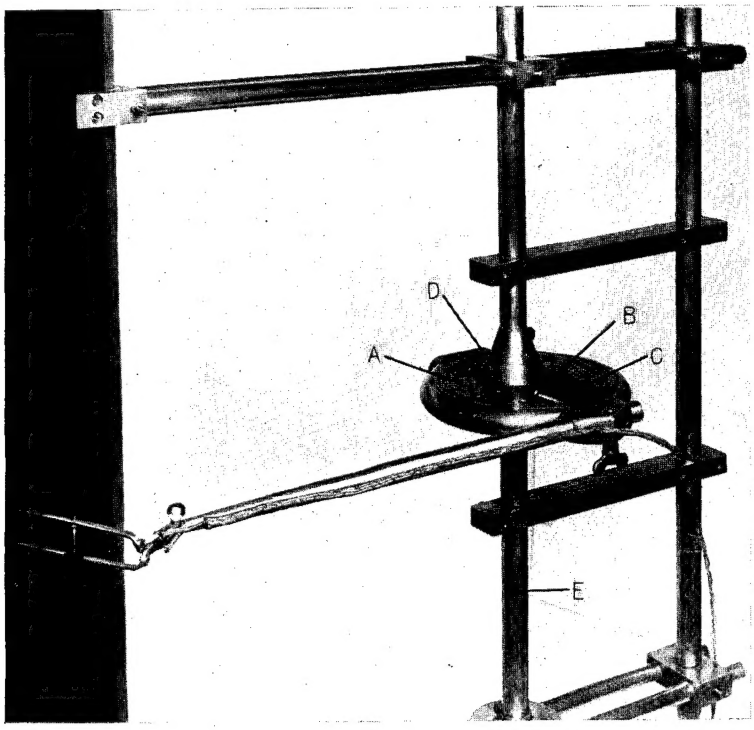

FIGURE 1.—Photograph showing details of hot-wire anemometer and traversing equipmet. A, micrometer carriage; B, fixed way; C, micrometer screw, D, housing; E, tubular member.

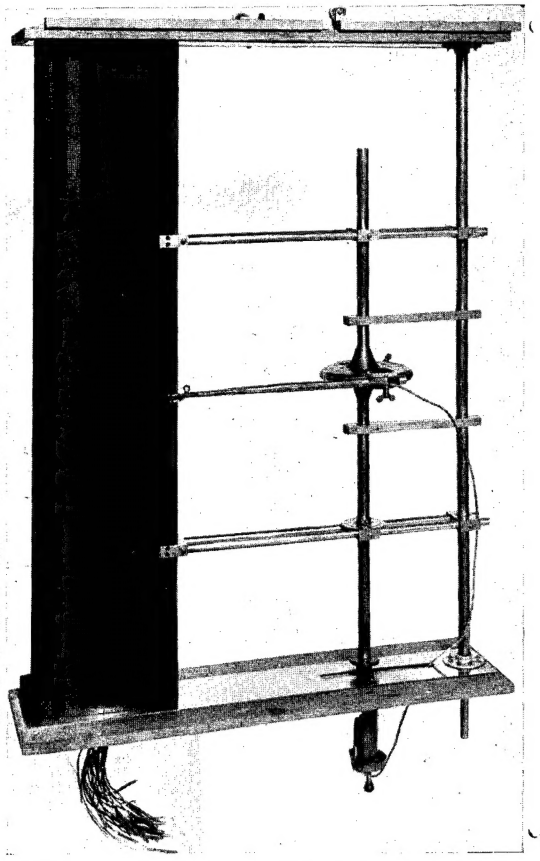

FIGURE 2.—Photograph showing over-all view of elliptic cylinder and traversing equipment.

The work was conducted at the National Bureau of Standards with the cooperation and financial assistance of the National Advisory Committee for Aeronautics.

The author wishes to acknowledge his indebtedness to Dr. Hugh L. Dryden for many valuable suggestions, to W. H. Boyd for the design and construction of traversing equipment, and to W. C. Mock, Jr., for his assistance with the experimental program.

DESCRIPTION OF ELLIPTIC CYLINDER, HOT-WIRE ANEMOMETER, AND TRAVERSING EQUIPMENT

THE ELLIPTIC CYLINDER

As stated in the introduction, the elliptic cylinder had major and minor axes of 11.78 and 3.98 inches, respectively, and was 4½ feet long. When mounted vertically in the wind tunnel, it extended completely from the upper to the lower face of the octagonal working section. The cylinder was made of wood, and had a smooth surface obtained by alternate varnishing and sandpapering and finally polishing with crocus paper. Twenty-one pressure orifices were inserted in the cylinder 2½ inches below the center for obtaining the pressure distribution over the surface. Eighteen of the orifices were distributed around the side on which boundary-layer measurements were to be made, one was at the leading edge and two were placed on the opposite side near the leading edge to aid in alining the cylinder with its major axis parallel to the wind direction. Only this position was used in the investigation.

HOT-WIRE ANEMOMETER AND TRAVERSING EQUIPMENT

Speed measurements in the boundary layer were made with a hot-wire anemometer consisting of a fine platinum wire mounted on the end of a pair of prongs through which an electric current could be passed to heat the wire. The particular arrangement of the anemometer used for the measurement of mean speeds is shown with the traversing mechanism in figure 1. The requirement that the prongs and the mounting be rigid enough to withstand deflection in the wind and still cause no measurable interference led to the arrangement shown, in which the traversing assembly was placed downstream from the cylinder. The distance from the trailing edge of the cylinder to the nearest point of the micrometer carriage A was 14 inches. In order to

prevent accidental movement between the cylinder and the wire, the cylinder and the traversing equipment were rigidly attached to two end boards, the entire assembly forming the unit shown in figure 2. When the unit was placed in the tunnel, the end boards were fitted into two rectangular openings in the tunnel walls.

Interference from the prongs themselves was made negligibly small by tapering and by using fine steel needles about 1 inch long to form the ends. There still remained a troublesome flow disturbance caused by the wire itself, when an attempt was made to use the customary 0.002-inch-diameter wire. It turned out to be necessary to use a wire 0.00063 inch in diameter and to limit its length as much as possible. Even with the smaller size of wire some interference persisted, as evidenced by a slight shift in the position of separation back of the wire when the wire was in some upstream part of the boundary layer.

Traversing of the wire through the boundary layer was accomplished by movement of carriage A with respect to the fixed ways B shown in figure 1. In this arrangement the micrometer screw C was fixed to the carriage and the two were propelled together by a nut inside housing D. The nut was rotated by bevel gears from which a shaft extended to the outside of the tunnel through the tubular member E. Carriage A could be rotated about E as an axis to permit traversing along any normal to the surface of the cylinder.

DETERMINATION OF MEAN SPEED

In the measurement of mean speed with the hot-wire anemometer, the method known as the "constant temperature method" was used; that is, the current through the wire was varied with the speed so as to maintain the wire at some fixed temperature above that of the surrounding air. The electric circuit was arranged so that the wire formed one arm of a Wheatstone bridge. With a very small bridge current, the cold resistance of the wire was measured. Then the resistance of the opposite arm of the bridge was increased by a definite amount and a balance of the bridge was again obtained by increasing the bridge current until the wire resistance increased through heating by the amount of the added resistance. In this way a definite temperature rise was maintained by the bridge. If E is the voltage drop across the wire and R is its resistance, then by the well-known hot-wire equation due to King (reference 2), the heat loss E^2/R may be expressed as a function of the air speed, the dimensions of the wire, the temperature rise, and the properties of the air. King's equation is useful to show the quantities upon which the heat loss depends but cannot be relied upon to determine the absolute value of the speed. Hence calibration of the instrument at known speeds is necessary. Using the present procedure, readings of E on a potentiometer and of R on the Wheatstone bridge served, with a calibration curve, to determine the speed.

Frequent calibrations were made necessary by a steady change with use in the cooling properties of the wire. The cause of this change was found to be the gradual accumulation of very fine dust from the air on the upstream side of the wire. When the cause was discovered, precautions were taken to suppress dust as much as possible. This precaution improved the conditions somewhat but frequent calibration was continued. Changes in the density and the thermal conductivity of the air, upon which the heat loss also depends, were never large enough to cause any detectable change from one calibration to another.

HEAT LOSS TO THE SURFACE

A disadvantage of the hot-wire anemometer, when applied to the measurement of speed very near to a surface, is the error caused by heat loss from the wire to the surface. The error, causing the speed to appear too high, becomes greater the nearer the surface the measurement is made. Several investigators have endeavored to determine the heat loss to the surface by conducting an experiment in still air at several wire temperatures to find the difference between the rate of heat loss near the surface and that far from the surface. In this manner the heat loss is found as a function of the wire temperature and the distance from the surface. Dryden (reference 3) found the heat loss to an aluminum plate to be given empirically by

$$H_p = 1.27 \times 10^{-8} \frac{l}{y} \theta^2 \qquad (1)$$

where H_p, is the heat loss to the plate, watts.
l, the length of the wire, inches.
y, the distance from the plate, inches.
θ, the temperature difference between the wire and the plate, degrees C.

A similar relation with the constant roughly 1.0×10^{-8} was found for a varnished wooden surface in the earlier work on the elliptic cylinder.

From the obvious error often introduced by applying the correction, corrections based on such determinations made in still air are known to be much too large for moving air. Needless to say, it would be very difficult to determine a heat-loss correction for moving air that would apply under all conditions.

In view of these difficulties, a procedure that obviated the need for heat-loss corrections was adopted in the present work. By equation (1), the heat loss to the surface is proportional to θ^2 and, by King's hot-wire equation, the heat loss to the air is proportional to θ. Obviously, the smaller θ is made, the less is the amount of the heat lost to the surface relative to that lost to the air. The procedure adopted was to make θ small enough so that the heat lost to the surface was insignificant compared with that lost to the air. Using several values of θ, measurements of the speed were made in that part of the boundary layer where the speed near the surface was low, and it was found that values of θ

as high as 150° C. caused no measurable error. How much higher the allowable value of θ might have been was not determined, since 150° C. was sufficient to give the desired sensitivity at the highest speed.

DETERMINATION OF SPEED FLUCTUATIONS

The measurement of speed fluctuations with the hot-wire anemometer required a technique considerably different from that described. The problem here is one of measuring variations in speed from the mean, when such variations occur with frequencies ranging from a few cycles per second to over 1,000. Only variations in magnitude of the velocity are considered here because the cooling of a simple hot wire does not respond to changes in direction. Hence the term "fluctuation" refers to an increase or a decrease in the instantaneous speed only. The fluctuations vary the wire temperature and hence the voltage drop across the wire; and, when the relation between speed change and voltage change is known, the voltage fluctuations serve as a measure of the speed fluctuations. The important features of the wire are fineness, to reduce lag arising from thermal capacity, and shortness, to reduce the error caused by variations in the instantaneous value of the fluctuations from point to point. The shortness requirement limits the magnitude of the

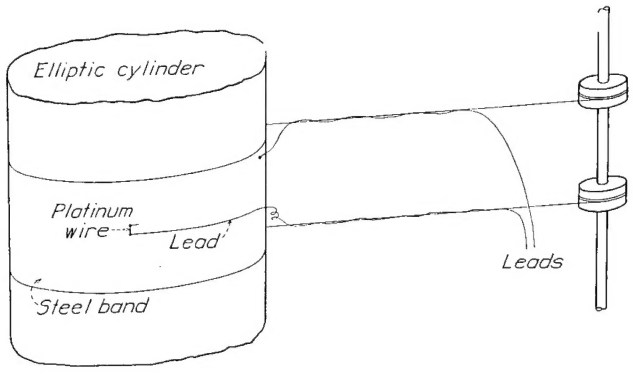

FIGURE 3.—Diagram of sliding band carrying hot wire.

voltage fluctuations and makes it necessary to amplify the voltages before they can be measured.

The amplifier used was the one described in reference 4. A compensating circuit is incorporated in the amplifier by which it is possible to compensate for the lag of the hot wire, if the diameter of the wire is not too large. The range of compensation was such that a wire 0.00063 inch in diameter could be used and the over-all gain of the amplifier was sufficient to allow the length of the wire to be reduced to about 0.15 inch. The wire was then of the same diameter as that used for measuring mean speeds but was only about one-seventh as long.

In this case, the mean value of the heating current rather than the mean temperature, was kept constant at all speeds and the voltage fluctuations were read on a thermal-type milliammeter connected to the output of the amplifier. The calibration consisted in measuring the mean voltage at different speeds with the same constant value of the current. The method of using the calibration to calculate the root-mean-square of the speed fluctuations is described in reference 5. The lag characteristics of the wire and the adjustment of the compensation were calculated by the method described in reference 6. With the correct compensation, the over-all response of wire and amplifier was uniform from 3 to 1,000 cycles per second. Most of the fluctuations fall within this range.

When details of the fluctuations such as wave form and frequency were to be studied, a cathode-ray oscillograph was connected to the output of the amplifier and the screen photographed with a moving-film camera.

HOT WIRE MOUNTED ON SLIDING BAND

In the course of the experiment the advantage of being able to move the hot wire around the contour of the ellipse at a small fixed distance from the surface became apparent. The need for doing so first arose when it became necessary to follow the changes in mean speed from point to point about the surface in order to detect transition. After several attempts to use a modification of the traversing equipment and the hot-wire anemometer shown in figure 1 had proved unsuccessful owing to the difficulty of keeping the distance between the wire and the surface constant, the scheme of placing a hot wire on a sliding band attached to the cylinder was tried. A strip of sheet steel 0.002 inch thick and 6 inches wide was fitted about the elliptic cylinder in such manner as to make a snugly fitting band capable of being slipped around the cylinder and remaining in any desired position. The arrangement is shown in figure 3. At the center of the band a short length of platinum wire of the usual 0.00063-inch diameter was mounted parallel to the surface and normal to the direction of flow. One end of the wire was soldered to a fine copper lead cemented to the surface and suitably insulated and the other was soldered to a short lead of the same diameter grounded to the band. The spacing between the platinum wire and the surface was usually 0.008 inch. In order to slip the band about the surface from the outside of the tunnel, two steel wires were attached to the band on the side opposite the platinum wire and were run to pulleys and shaft, as shown in figure 3.

The disturbance caused by the band was investigated by coating the surface with a mixture of kerosene and lampblack and noting the pattern produced in a wind of about 60 feet per second. While using the kerosene- and lampblack-method to investigate separation, it was found that the lampblack not only showed the position of separation but also afforded a very sensitive indication of the presence of small particles of dirt on the

surface by the distortion produced in the line of accumulated lampblack at separation. With the band in place, the line showed small kinks at the edges of the band and a third kink at the center caused by the wire. Since the general course of the line was the same as for the bare cylinder, it was concluded that the disturbance was of no consequence.

The present arrangement turned out to be useful in the study of speed fluctuations as well as of mean speeds. The only modification required in the general scheme was the replacement of the grounded lead with an insulated lead to avoid troubles from a double ground.

METHOD OF PRESENTING OBSERVATIONS

Before the elliptic cylinder was installed in the tunnel, a standard pitot-static tube was placed at the position to be occupied by the leading edge of the cylinder and the speed was determined for this position in terms of the pressure at a tunnel-wall orifice about 8 feet upstream. The pressure at this orifice was then used to calculate the speed when the cylinder was in the tunnel. This speed, denoted by U_0, is therefore the speed which would prevail in the tunnel with the cylinder absent and, consequently, may be regarded as the speed of the undisturbed stream.

The actual speed near the cylinder (in the potential region just outside the boundary layer) may be computed from the pressure distribution over the cylinder as follows:

The dynamic pressure q for the undisturbed stream is defined by $q=\frac{1}{2}\rho U_0^2$, where ρ is the air density. If p_s is the static pressure of the undisturbed stream and p_t is the total pressure (a constant everywhere in the potential region), q may be expressed also as $q=p_t-p_s$. The pressure on the surface, which was determined by pressure orifices in the cylinder, is denoted by p. Since the pressure is assumed to remain constant across the boundary layer, p may be regarded as the static pressure in the potential region just outside the boundary layer and is therefore related to U, the speed just outside the boundary layer by

$$p_t-p=\frac{1}{2}\rho U^2$$

The pressure distribution about the cylinder is given in terms of $p-p_s$ and is expressed nondimensionally by $(p-p_s)/q$. Likewise the speed at the outside of the boundary layer is expressed nondimensionally by U/U_0 and is obtained from the pressure distribution by

$$\left(\frac{U}{U_0}\right)^2=\frac{p_t-p}{q}=\frac{p_t-p_s-(p-p_s)}{q}=1-\frac{p-p_s}{q}$$

Lengths, specifying position on the surface or in the boundary layer, will generally be expressed nondimensionally in terms of D, the minor axis of the ellipse. The Reynolds Number of the cylinder is defined by

$$R=\frac{U_0D}{\nu}$$

where ν is the kinematic viscosity.

The speed fluctuations both in the boundary layer and in the free stream will be termed "u-fluctuations" in order to denote the component of the fluctuation in the direction of mean flow. The root-mean-square value of u-fluctuations will be denoted by u' and will always be expressed nondimensionally as u'/U_0. In the free stream and in the turbulent part of the boundary layer, u'/U_0 will be termed the "intensity" of the turbulence. The term "percentage turbulence," to express $100\,u'/U_0$, is in common usage in the literature and will be used in the same sense here.

The scale of the turbulence will be denoted by L and is defined by

$$L=\int_0^\infty R(z)dz$$

where $R(z)$ is the coefficient of correlation between instantaneous values of two u-fluctuations separated by the cross-stream distance z. For a more complete discussion of L and of the relation between $R(z)$ and z the reader is referred to reference 7.

SYMBOLS

D, minor axis of ellipse (3.98 inches), used as the reference length.
U_0, speed of the undisturbed stream, feet per second.
R, Reynolds Number U_0D/ν.
q, dynamic pressure of the undisturbed stream $\left(\frac{1}{2}\rho U_0^2\right)$.
p/q, dimensionless pressure on surface of cylinder.
p_s/q, dimensionless static pressure in undisturbed stream.
x/D, dimensionless distance from the leading edge to any point on the surface.
y/D, dimensionless distance from the surface measured along the normal.
δ, boundary-layer thickness.
δ/D, dimensionless boundary-layer thickness.
U/U_0, dimensionless speed in the potential region just outside the boundary layer.
u/U_0, dimensionless speed in the boundary layer.
u', root-mean-square value of the u-fluctuations.
u'/U_0, fluctuation intensity or intensity of turbulence.
L, scale of turbulence.
t, turbulent boundary layer.
S, S_t, separation points.
τ, shearing stress.
l, mixing length.

BOUNDARY-LAYER PHENOMENA AT LOW STREAM TURBULENCE

PRESSURE DISTRIBUTIONS

As pointed out in the introduction, pressure distributions were determined about the elliptic cylinder in order to find an air speed for which the boundary layer over the rear part of the cylinder would be turbulent. Since the turbulence normally prevailing in the wind-tunnel stream was 0.85 percent and the critical Reynolds Number of a 5-inch sphere was 268,000, it seemed that such a condition would be found well below the maximum speed attainable in the tunnel. By a determination of the pressure distribution at different speeds, a critical region like that of spheres was found for the elliptic cylinder extending from about 15 to 55 feet per second. The change in the pressure distribution occurring through this region is shown by the several curves of figure 4. The curves for 11.2 and 70.0 feet per

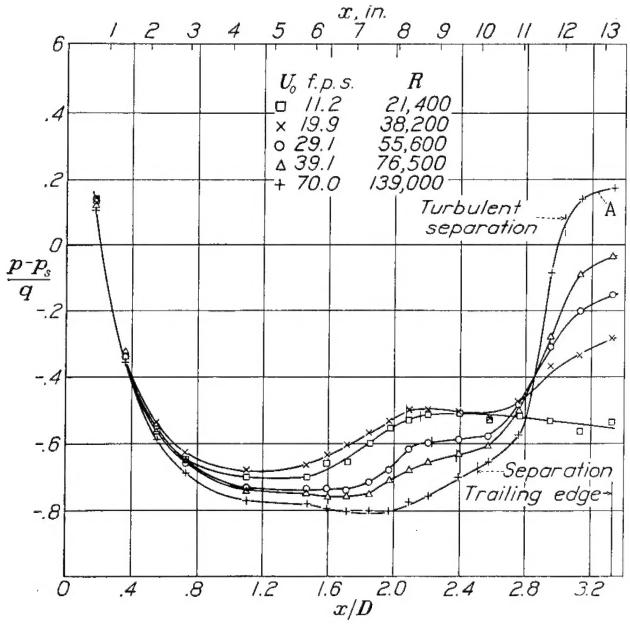

FIGURE 4.—Pressure distribution around one side of elliptic cylinder. Stream turbulence, 0.85 percent.

second represent the two invariable forms occurring below and above the critical region. The term "invariable" is used here in a restricted sense to mean fixed or showing very little change over a certain speed interval. The lower-speed type would certainly change for extremely low speeds and the same is true of the higher-speed type, if the speed were made sufficiently high. The speed was not carried high enough to determine where a change would occur in the distribution above the critical region. No observable change could be found in the distribution shown for 70.0 feet per second from 60 to 80 feet per second.

SEPARATION STUDIES

As indicated in figure 4, the change in the pressure distribution was accompanied by a change in the point at which the boundary layer separated from the surface. The method of detecting separation was the well-known one of applying a mixture of kerosene and lampblack to the surface and then running the tunnel at the desired speed for a sufficient length of time for the surface drag to establish a flow pattern. The vertical position of the cylinder was well adapted to this method because only the frictional drag of the air tended to carry the mixture horizontally. Downward drainage along the surface occurred, of course, but was a distinct advantage in that it reduced the film thickness, thus preventing flow under pressure gradient and, in addition, indicated the direction of the surface friction by the inclination of the drainage lines.

After the flow pattern was established and the kerosene had partly evaporated, a record of the pattern was easily made by pressing a piece of white paper against the surface. Figure 5 shows three such records made at 25, 43, and 70 feet per second. It will be noted that the patterns on the upstream part of the surface show a surface drag in the direction of the stream, indicated by the inclination of the streaks, which is followed by a region of stagnant air where the streaks are vertical. Although not clearly shown in the figure, it was usually possible to find a third region of short length just back of the stagnation region in which the streaks were inclined forward, giving evidence of reverse flow. Separation was assumed to occur in the stagnation region.

Because of the rearward movement of separation with increasing speed, it was at first assumed that the boundary layer became turbulent ahead of separation and that separation of a turbulent layer was being observed. This interpretation sufficed for patterns A and B, but not for C, where a second line of separation was found at the point marked S_t. This double separation, illustrated by C, was a characteristic of the flow above the critical region and always occurred at the same points on the surface. It was not until speed distributions had been determined throughout the layer with both high and low stream turbulence and studies of transition had been made with different amounts of turbulence that a satisfactory explanation of this phenomenon was afforded. The boundary layer was found to maintain the general aspects of a laminar boundary layer up to separation, but in no case was it purely laminar at the separation point above 15 or 20 feet per second because of a faint beginning of transition near the 6-inch position. Patterns A and B of figure 5 therefore show the separation of a "nearly laminar" layer. In pattern C the first separation at S is also the separation of a nearly laminar layer and the second at S_t is that of a turbulent layer, a complete transition having occurred in the free layer between S and S_t and the resulting turbulent layer having reattached itself to the surface. As indicated in the figure, the first separation began at 10 inches, and the final turbulent separation occurred at 12.05 inches.

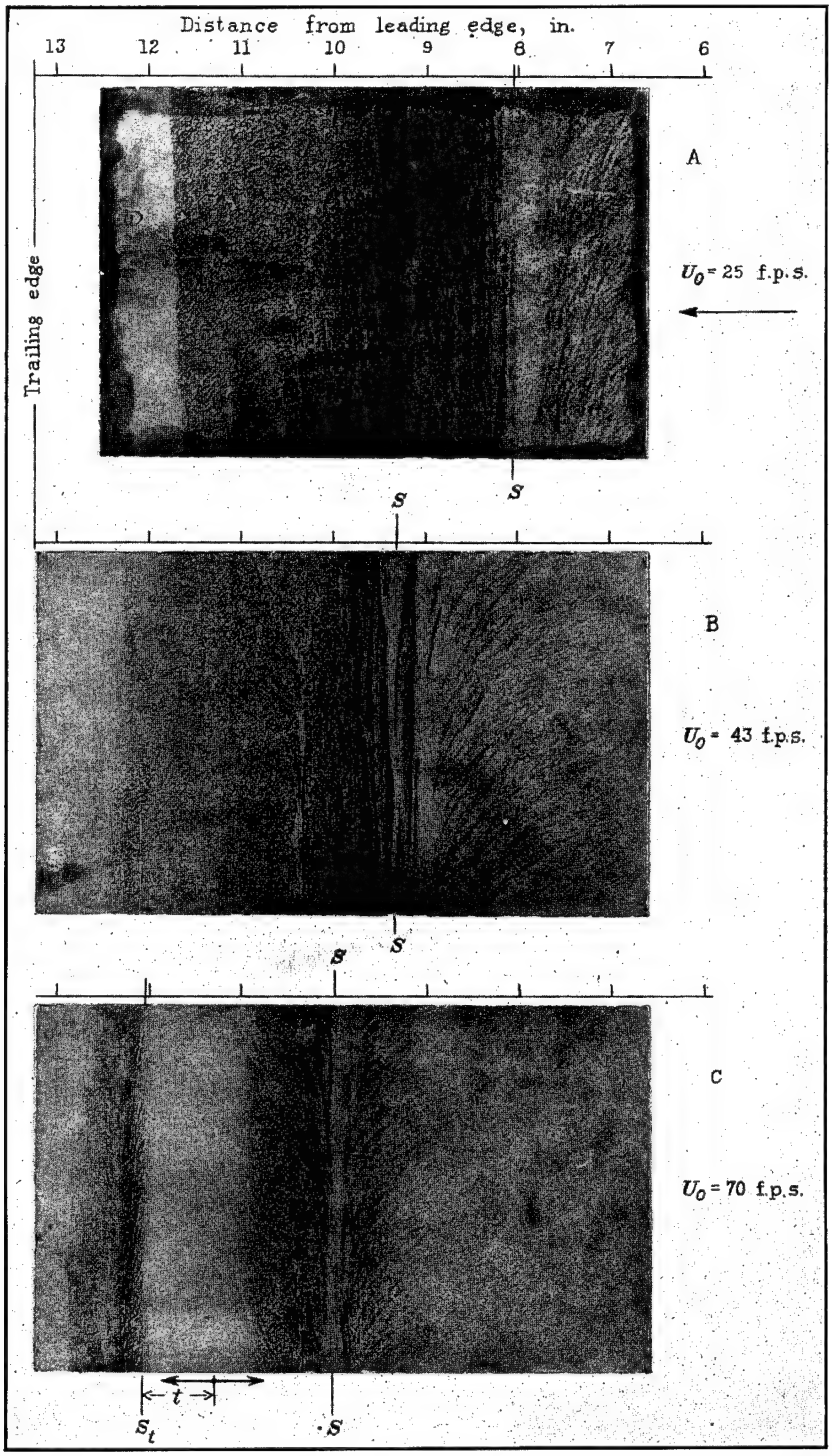

FIGURE 5.—Kerosene and lampblack patterns showing movement of separation with speed and development of reattached turbulent layer. Stream turbulence, 0.85 percent. Distances were measured along surface. S, S_t=separation points, t=Turbulent boundary layer. Arrows indicate direction of flow.

The direction of flow in the separation region of pattern C and the extent of the region were obtained by a second method of detecting separation that proved to possess certain advantages over the kerosene-and-lampblack method. The procedure was to apply to the surface a concentrated water solution of litmus, which was then reddened by fumes of hydrochloric acid and allowed to dry. Then, with a wind of the desired speed, a small amount of ammonia gas was released at the surface through a hypodermic needle in the neighborhood of the point to be investigated. The direction of the flow was clearly indicated by the blue color of the litmus. This method gave a definite indication of the direction of flow in the low-speed regions about separation points and showed details of the air motion impossible to obtain with the kerosene- and lampblack-method. In this way the first separation region was found to extend from 10 inches to 11.2 inches, as indicated in figure 5.

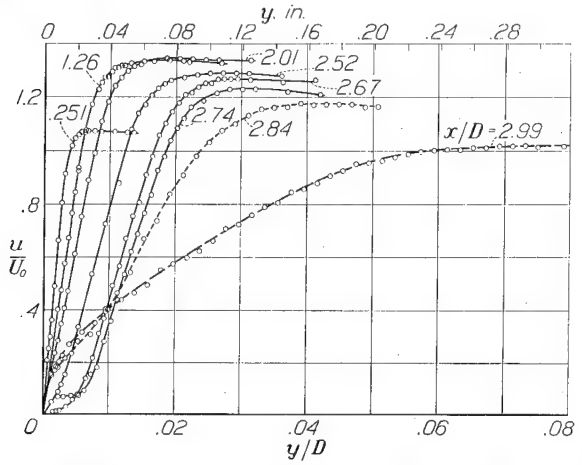

FIGURE 6.—Speed distribution in boundary layer of elliptic cylinder. Air speed (U_0), 70 feet per second; R, 139,000; stream turbulence, 0.85 percent.

MEAN-SPEED DISTRIBUTION IN THE BOUNDARY LAYER

Traverses normal to the surface of the elliptic cylinder were made with the hot-wire anemometer to determine the speed distribution in the boundary layer at 15 positions about the surface, beginning 1 inch from the leading edge and ending at 12.6 inches. In terms of x/D, in which positions on the surface will generally be expressed, the traverses were begun at 0.251 and ended at 2.99. In all cases the speed of the stream U_0 was 70 feet per second, corresponding to a Reynolds Number of the cylinder of 139,000.

Several of the speed distributions are shown in figure 6. It will be observed that the profiles from $x/D=0.251$ to 2.01 show little change other than that caused by a thickening of the boundary layer and all have the shape generally found in a laminar boundary layer. At 2.52 the profiles show the beginning of separation. From 2.67 to 2.74 the very small initial slope of the curves shows that separation has occurred. Between 2.74 and 2.84 a marked change has occurred, since all evidence of separation has disappeared at 2.84. The profile at 2.99 is certainly not that ordinarily ascribed to a laminar boundary layer, neither does it have the characteristics found in a turbulent boundary layer of a flat plate where the customary ⅐-power law represents the speed distribution. As pointed out by Fediaevsky in reference 8, however, an adverse pressure gradient has a marked effect on the turbulent-speed profile. If the nature of this effect is considered and the strong adverse gradient existing at 2.99 is noted, it can be said that the profile is characteristic of a turbulent boundary layer.

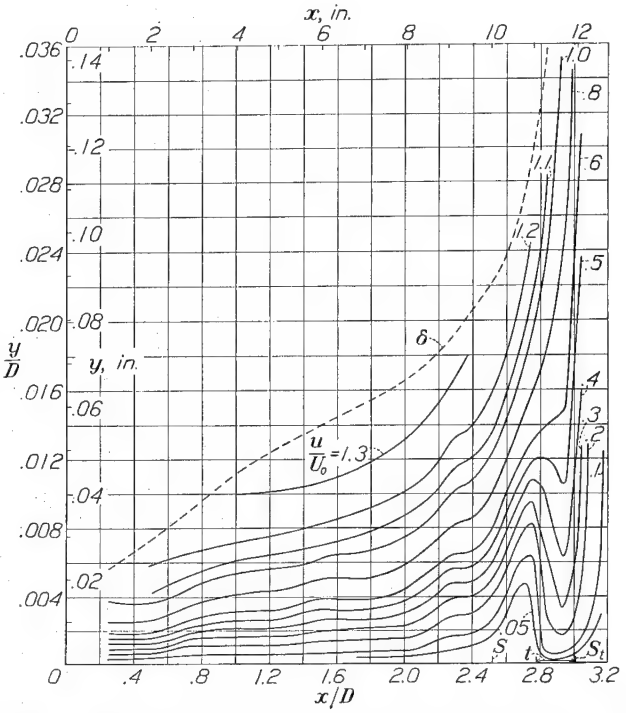

FIGURE 7.—Contours of equal speeds in boundary layer of elliptic cylinder. Air speed (U_0), 70 feet per second; R, 139,000; stream turbulence, 0.85 percent.

A picture of the boundary layer as a whole may best be obtained from the contour diagram of figure 7, where each curve represents a particular value of u/U_0. The dotted curve shows the boundary-layer thickness δ, which is here defined as the value of y where $u/U_0=0.995\ U/U_0$. The occurrence of a separation followed by a reattachment of the layer to the surface is evidenced by the hump in the contours from $x/D=2.5$ to 2.9. The approach to separation of the turbulent layer is shown by the very rapid increase in slope of the curves beyond the hump. Owing to the fact that the hot wire is insensitive to direction of flow, the measurements are not exact in the immediate vicinity of separation and hence neither figure 6 nor figure 7 serves to locate accurately the separation. The separation points and the extent of the turbulent layer were therefore obtained from figure 5. The values of x/D at S and S_t are, respectively, 2.51 and 3.03. The attached turbulent layer extends from 2.81 to 3.03.

The chief function of figures 6 and 7 is to show the

condition of the boundary layer upon separation—whether laminar or turbulent. By inspection it would be concluded from figure 6 that the boundary layer was laminar at the first separation point and turbulent at the second. Mere inspection is, however, rather inadequate because the conclusion depends on the judgment of the observer. A far better criterion of the state of the boundary layer would be provided by a comparison of observed speed distributions and positions of separation with these same quantities computed by boundary-layer theory. At present, existing solutions involve approximations whose validity is usually tested by comparison with experiment. Hence such solutions may not be relied upon for accurately defining the type of boundary layer found by experiment. With full recognition of the weakness of the procedure, certain simple comparisons with theory will be made in an effort to throw a little additional light on the problem.

In the von Kármán-Pohlhausen theory of the laminar boundary layer (reference 9) the criterion for separation is that the parameter $\frac{dU}{dx}\frac{\delta^2}{\nu}$, usually denoted by λ, shall have the value -12 at the separation point. Using the pressure gradient and the boundary-layer thickness observed at the first separation point, λ was computed to be -11.8. This value is in excellent agreement with theory and strongly supports the view that the separation at 2.51 is of the laminar type.

The von Kármán-Millikan theory (reference 10) has shown considerable promise in the solution of the laminar boundary-layer problem and has been used by von Doenhoff (reference 11) to calculate the separation point on the elliptic cylinder used in the present work for the perfect-fluid pressure distribution. In order to obtain a result applicable to actual conditions, the observed pressure distribution must be used. It so happens that the curve for the perfect-fluid pressure distribution fits the observed pressures (curve A, fig. 4) so closely up to $x/D=2.8$ that no better smoothed curve could be drawn. Since the method of solution requires, in effect, that the pressure distribution be fitted by a smoothed curve, von Doenhoff's solution may be regarded as the best possible. The computed separation point is 2.38. In view of the approximations involved in the theory and its application, the agreement with the observed separation at 2.51 must be considered good. Theory therefore supports the general impression given by figures 6 and 7 that the first separation is of the laminar type.

In order to test the second separation, turbulent boundary-layer theory might be applied to the reattached layer. This method was not believed to be worth while, however, in view of the limited length of the boundary layer and the unusual conditions under which it was formed. As has been pointed out, theory offers no completely satisfactory criterion even under the best circumstances.

It is well, therefore, to examine further experimental evidence that may contribute information as to the nature of the layer.

SPEED FLUCTUATIONS IN THE BOUNDARY LAYER

In the investigation of the boundary layer near a flat plate (reference 3), Dryden found speed fluctuations (u-fluctuations) in the laminar boundary layer having amplitudes as great as those in the turbulent part of the layer. On the mere existence of fluctuations alone it was therefore impossible to distinguish between the turbulent and the laminar parts of the boundary layer.

It is generally recognized that the fundamental difference between the fluctuations in turbulent and laminar parts of the boundary layer is one of correlation between the u-fluctuations and the v-fluctuations, the v-fluctuations being those occurring normal to the surface. If the instantaneous values of u- and v-fluctuations are denoted by u_i and v_i, respectively, the essential difference may be expressed in terms of the value of $\overline{u_i v_i}$, where the bar denotes average value. The turbulent shearing stress is given by $\rho\,\overline{u_i v_i}$. A turbulent shearing stress must be absent in a laminar boundary layer and $\overline{u_i v_i}$ must be zero. By definition, a turbulent or partly turbulent layer is one in which a turbulent shearing stress exists, that is, where $\overline{u_i v_i}$ has a value other than zero. The value of $\overline{u_i v_i}$ therefore furnishes the best criterion as to the turbulent or the laminar condition of the layer.

With the simple hot-wire anemometer used by Dryden, it was impossible to determine $\overline{u_i v_i}$. The experimental difficulties attending such a measurement appear to be very great, especially in a thin boundary layer, and no means of doing so was found in the present investigation. Dryden has shown, however, in reference 3, that the simple hot wire does reveal an important difference between the fluctuations in the two parts of the boundary layer, namely, that the average frequency of the fluctuations is much greater in the turbulent than in the laminar boundary layer. On the flat plate, transition occurred quite abruptly and the position of transition was clearly defined by the marked difference in frequency on its two sides.

An effort was made in the present investigation to see whether a similar condition existed on the elliptic cylinder and, in particular, to determine whether the frequency of the fluctuations would serve to distinguish between the turbulent and the laminar parts of the layer. Accordingly, with a hot wire attached to the sliding band as previously described, records of the fluctuations were made by photographing the screen of a cathode-ray oscillograph connected to the output of the compensated amplifier. The wire was 0.00063 inch in diameter and 0.18 inch long and was attached to the band at a fixed distance of 0.0158 inch from the surface.

Figure 8 shows several of the records obtained at

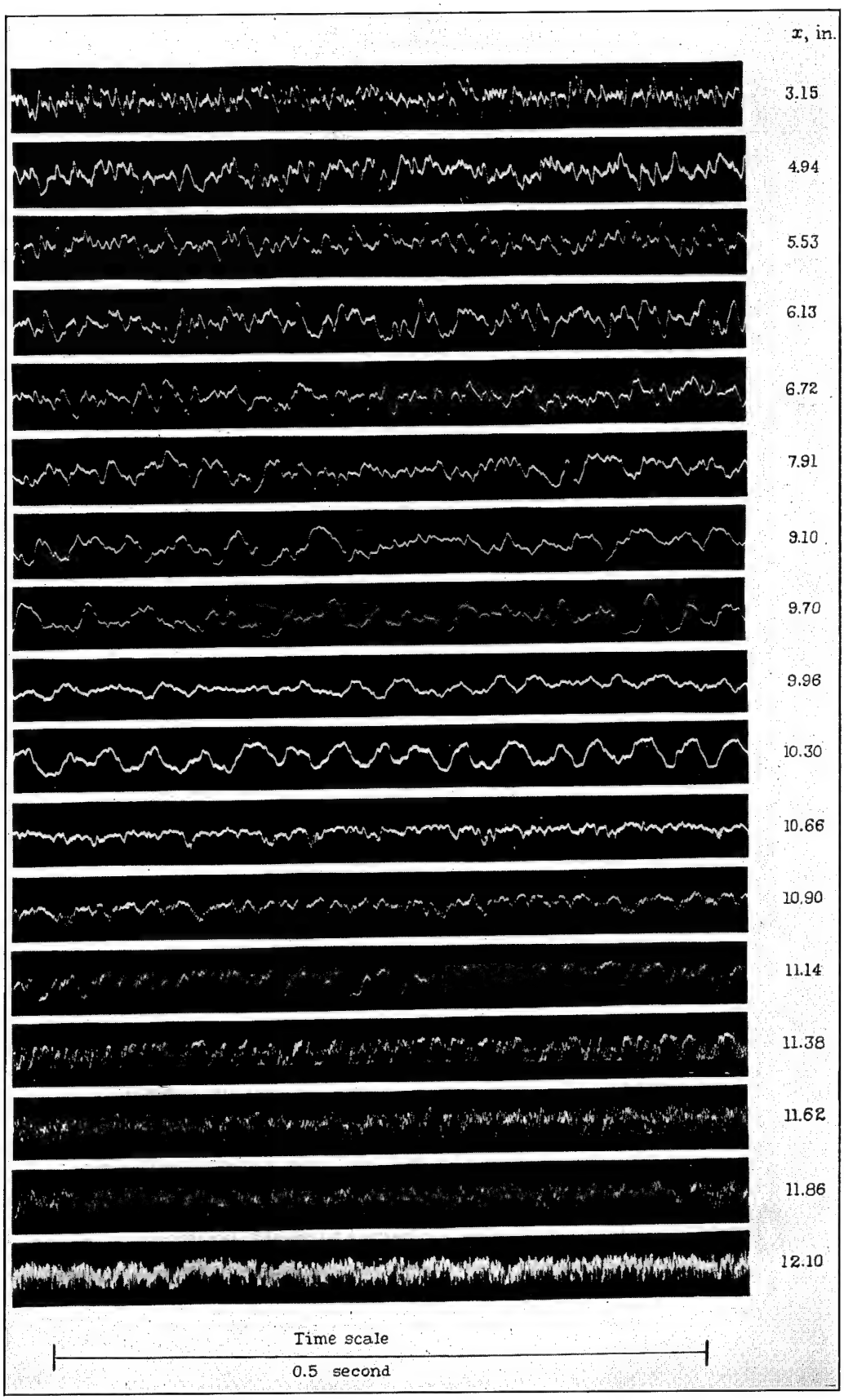

FIGURE 8.—Oscillograph records of u-fluctuations in boundary layer at 0.0158 inch from surface. Obtained with hot wire on sliding band. Air speed (U_0), 70 feet per second; stream turbulence, 0.85 percent.

different positions about the surface. It is immediately evident that the frequency is much higher throughout the reattached layer, beginning near 11.14 inches, than in any other parts of the layer. No noticeable change has occurred in either the general character of the wave or the frequency up to $x=9.10$ inches. Beyond this point, a regularity in the wave has begun to develop, which persists through the first separation region. In the record at 10.30 inches, situated near the center of the separation region, the regularity is quite marked, having a frequency of about 32 cycles per second. It is interesting to note that the fluctuations are everywhere quite random except through the separation region. The regular fluctuations are believed to be due to a slight fore-and-aft oscillation of the separation point, caused perhaps by pressure pulsations from the vortex street in the rear of the cylinder.

Owing to the absence of any perceptible increase in frequency with distance from the leading edge until the reattached layer is reached, it would be concluded by analogy with Dryden's results on the flat plate that transition to a definitely turbulent layer occurred in the separation region. With no evidence of transition ahead of the first separation point it appears from all the tests applied thus far that laminar separation occurred at $x/D=2.51$. This was the general conclusion drawn by the author before a more detailed study of transition had been made with different amounts of stream turbulence. In anticipation of some of the results to be given later, it may be stated that a gradual and incomplete transition may occur without any noticeable change in the frequency of the fluctuations and that conclusions drawn from the nature of the fluctuations may be in error in such cases. In the following sections it will be shown that the sliding band and the hot wire arranged to detect changes in the average speed near the surface affords a more sensitive means of detecting transition than any yet employed. Using this device to examine the boundary layer, it was found that a weak and very incomplete transition began at $x/D=1.53$, or very near the 6.1-inch position. The boundary layer has therefore separated at 2.51, not as a purely laminar layer but as a transition type with transition so incomplete that the layer continues to exhibit most of the properties of a laminar layer.

BOUNDARY-LAYER PHENOMENA AT HIGH STREAM TURBULENCE

When it was thus found impossible to obtain a complete transition without an intervening separation with the low turbulence normally prevailing in the tunnel, the stream turbulence was increased by placing a 1-inch-square-mesh wire screen 18 inches ahead of the leading edge of the cylinder. (See table I.) The intensity and the scale of the turbulence produced by this screen had been measured previously and reported in reference 7. Figure 9 gives results taken from this reference and shows the turbulent conditions prevailing at the position of the cylinder.

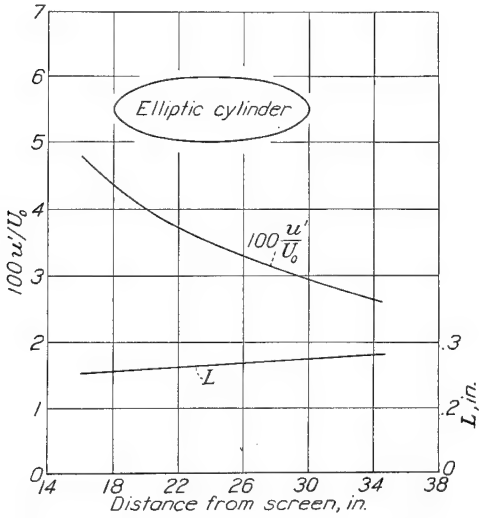

FIGURE 9.—Intensity and scale of stream turbulence produced by 1-inch mesh screen (from reference 7).

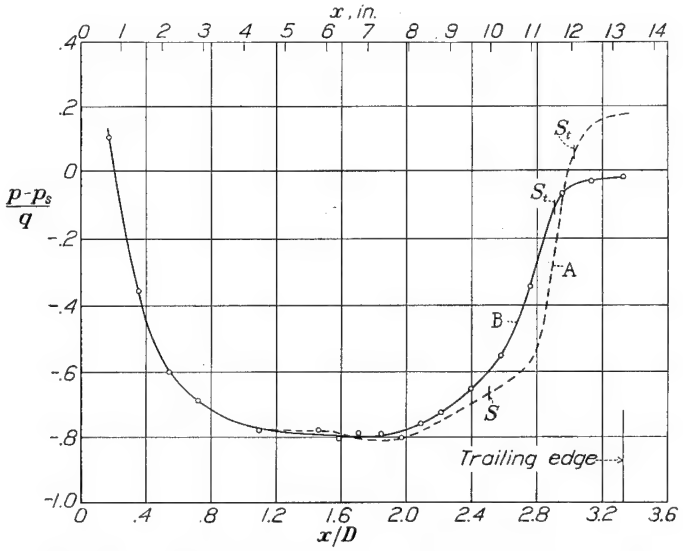

FIGURE 10.—Pressure distribution around one side of elliptic cylinder. Curve A—stream turbulence, 0.85 percent; air speed (U_0), 70 feet per second. Curve B—stream turbulence as shown by figure 9.

Kerosene-and-lampblack patterns made at various wind speeds showed a rearward movement of the separation point with increasing speeds up to 40 feet per second and no detectable movement for further speed increases. The final position of separation fell at $x/D=2.91$. Since the separation found at the lower turbulence was absent at all speeds with the higher turbulence, it was assumed that the transition occurred at a small value of x/D and that conditions were favorable for a study of a turbulent boundary layer of considerable length. A working speed of 60 feet per second, corresponding to a Reynolds Number of the cylinder of 118,000, was chosen for carrying out boundary-layer measurements.

Curve B of figure 10 shows the pressure distribution about the elliptic cylinder at 60 feet per second with the higher stream turbulence compared with curve A taken from figure 4. It will be observed that, even though each curve represents an invariable condition of the flow above the critical region, the two curves are different and the two turbulent separation points fall at slightly different positions.

MEAN-SPEED DISTRIBUTION IN THE BOUNDARY LAYER

At $U_0=60$ feet per second, traverses across the boundary layer were made with the hot-wire anemometer at 12 positions about the surface, beginning 1 inch from the leading edge and ending at 11.46 inches, 0.12 inch ahead of the separation point. The traverses at these extreme positions together with six traverses at intermediate positions are shown in figure 11. It is obvious that the distributions near the leading edge resemble those of a laminar boundary layer while those near the separation point resemble those of a turbulent layer but, because of the gradual change, it is impossible to tell just where transition has begun.

The corresponding contour diagram, giving curves of equal u/U_0, is shown in figure 12. This figure was prepared by making use of all the traverses and reading values of y from faired curves, like those shown in figure 11, for chosen values of u/U_0. Figure 12 shows

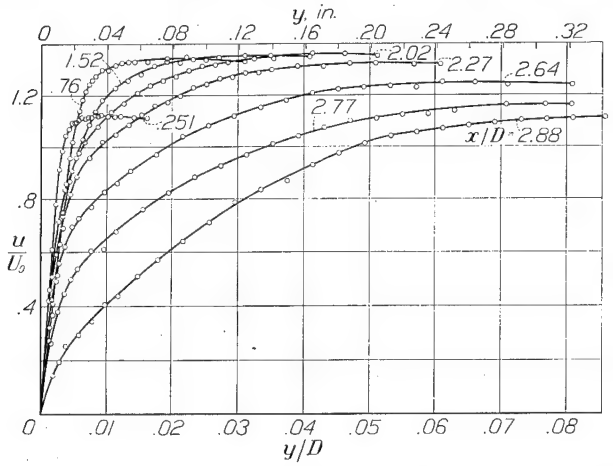

FIGURE 11.—Speed distributions in boundary layer of elliptic cylinder. Air speed (U_0), 60 feet per second; R, 118,000; stream turbulence as shown by figure 9.

the result of the change in type of distribution in such a manner that transition may be more easily recognized than in figure 11. The phenomenon usually associated with transition is found after $x/D=1.25$; that is, the bending of the contours toward the surface followed by an abrupt bending of the outer contours away from the surface. The bending away is due partly to the development of the turbulent boundary layer and partly to the approach to separation. It will be recalled by reference to figure 7 that a similar bending toward the surface, although considerably more abrupt, is caused by transition after separation and a reattachment of the layer to the surface. Although figure 12 shows that transition does take place, it fails to show where transition begins and ends. To bound the transition zone definitely requires a different treatment of the data or measurements of a different nature.

Again, testing by comparison with laminar or turbulent boundary-layer theory might be called into play; but the detection of small departures from the purely laminar or purely turbulent condition is made impossible by the approximate nature of the theories. For this reason it was believed useless to attempt to locate the beginning of transition by this procedure. It

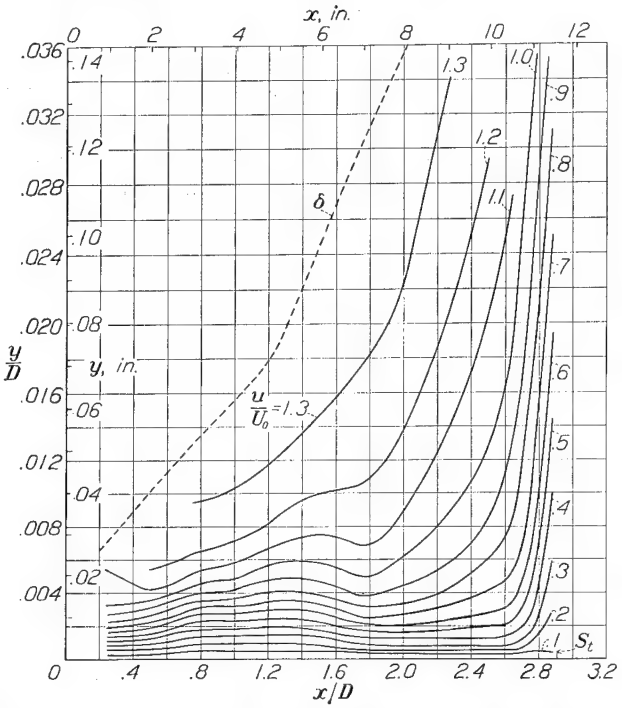

FIGURE 12.—Contours of equal speed in boundary layer of elliptic cylinder. Air speed (U_0), 60 feet per second; R, 118,000; stream turbulence as shown by figure 9.

appeared worth while, however, to compare the profiles back of $x/D=2$ with the usual $\frac{1}{7}$-power law and with the type of curve computed by the theory of Fediaevsky (reference 8) to aid in deciding whether the turbulent layer became fully developed before separation or whether the layer was still of the transition type when it separated.

Figure 13 shows speed distributions for $x/D=2.02$, 2.27, 2.64, 2.77, and 2.88 compared with that given by the $\frac{1}{7}$-power law. In the preparation of this figure, δ and U/U_0 were taken from figure 11 at the point where the slope of the curves is zero. Departures from the $\frac{1}{7}$-power law are to be expected, whether the layer is fully turbulent or not, where the adverse pressure gradient is great as at 2.64, 2.77, and 2.88. At 2.02 and 2.27, where the adverse pressure gradient is small, the departure can reasonably be attributed to incomplete transition, especially since the departure is in the direction to be expected if the layer here were partly laminar. It remains then to examine the effect

of pressure gradient on the distributions near the separation point.

The theory advanced by Fediaevsky in reference 8 is based on the fundamental relation

$$\tau=\rho l^2\frac{du}{dy}\left|\frac{du}{dy}\right| \tag{2}$$

in which τ is the shearing stress and l is the mixing length. The development by Fediaevsky differs from those by Prandtl and von Kármán, who have developed theories based on equation (2), in that the variation of l across the boundary layer is expressed by

$$\frac{l}{\delta}=0.14-0.08\left(1-\frac{y}{\delta}\right)^2-0.06\left(1-\frac{y}{\delta}\right)^4$$

and the variation of τ across the boundary layer is expressed by a power series of the form

$$\frac{\tau}{\tau_0}=A_0+A_1\left(\frac{y}{\delta}\right)+A_2\left(\frac{y}{\delta}\right)^2+A_3\left(\frac{y}{\delta}\right)^3+A_4\left(\frac{y}{\delta}\right)^4+\ \ldots\ .$$

where τ_0 is the shearing stress at the surface. Sufficient boundary conditions exist for the determination of A_0, A_1, A_2, A_3, and A_4, and their values are given as

$$A_0=1,\ A_1=\frac{\delta}{\tau_0}\left(\frac{\partial p}{\partial x}\right),\ A_2=0$$

$$A_3=-4-3\frac{\delta}{\tau_0}\left(\frac{\partial p}{\partial x}\right),\ A_4=3+2\frac{\delta}{\tau_0}\left(\frac{\partial p}{\partial x}\right)$$

When the substitutions for τ and l are made in equation (2), the differential equation for the speed distribution across the layer becomes

$$\frac{d\left(\frac{u}{U}\right)}{d\left(\frac{y}{\delta}\right)}=\frac{\sqrt{\frac{\tau_0}{\rho U^2}}\sqrt{1+A_1\left(\frac{y}{\delta}\right)+A_3\left(\frac{y}{\delta}\right)^3+A_4\left(\frac{y}{\delta}\right)^4}}{0.14-0.08\left(1-\frac{y}{\delta}\right)^2-0.06\left(1-\frac{y}{\delta}\right)^4} \tag{3}$$

It is shown in reference 8 that the expression for l/δ, although not universally true, is a fair approximation for a wide variety of pressure gradients. It is seen from the foregoing expressions for A_1, A_3, and A_4 that the effect of pressure gradient in the present theory is to influence the distribution of shearing stress. For a critical examination of the underlying concepts the original reference should be consulted.

By the use of values of δ obtained from figure 11, where the slope of the curves is zero, values of τ_0 obtained from the initial slope of the curves of figure 11, and values of $\frac{\partial p}{\partial x}$ from the slope of curve B in figure 10, A_1, A_3, and A_4 were evaluated for $x/D=2.77$ and 2.88. The integration of equation (3) was then carried out graphically to give the curves shown in figure 14. The differences between theory and experiment are greater than those found by Fediaevsky in his comparisons with the experimental curves obtained by Gruschwitz in the turbulent boundary layer of an airfoil. In one case, where the comparison was made near the beginning of the turbulent layer, a difference like that shown in figure 14 was found and the discrepancy was attributed to incomplete transition. Since neither τ_0 nor δ could be accurately determined in the present work, the effect of possible errors in these quantities was investigated. In no case could such errors account for more than a small part of the difference between the computed and the observed curves. It is probable, therefore, that separation occurred before the turbulent layer was fully developed.

Some investigators have associated the beginning of transition with the point of minimum skin friction (reference 12). This view seems reasonable when it is considered that the skin friction normally decreases as the boundary-layer thickness increases and only the introduction of turbulent shearing stresses can arrest the decrease or cause an increase in the skin friction. In an effort to locate the point of minimum skin friction, the local skin friction τ_0 was calculated from the initial slope of the speed-distribution curves of figure 11 and plotted as a friction coefficient against x/D in figure 15.

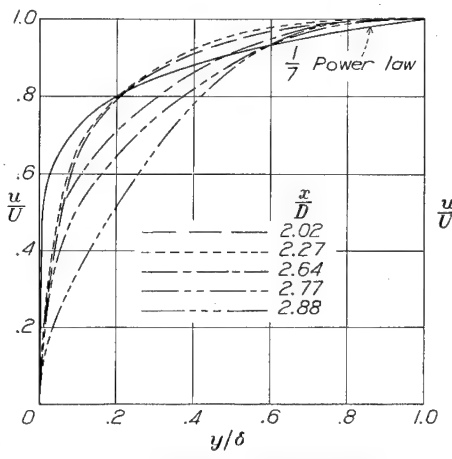

FIGURE 13.—Comparison of observed profiles with 1/7-power law.

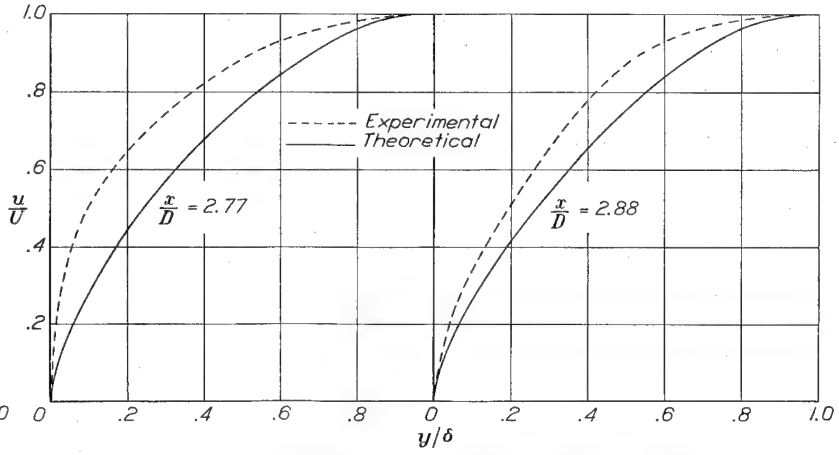

FIGURE 14.—Comparison of observed profiles with Fediaevsky theory.

A definite minimum exists, although the scatter of the points and the limited number of observations leave the position of the minimum rather indefinite. The final drop in the curve beginning at $x/D=2.2$ shows the effect of nearing the separation point.

To have obtained more values of τ_0 would have required more speed traverses at the expense of considerable time and effort. It proved to be quite easy, however, to follow the course of τ_0 by following the changes in speed from point to point at a small fixed distance from the surface with the sliding-band apparatus previously described. The essential conditions were that the distance from the surface remain fixed and small enough for the velocity gradient over that distance to be regarded as linear. A platinum wire 0.00063 inch in diameter and 0.5 inch long was fixed at the center of the band 0.008 inch from the surface, the arrangement being shown diagrammatically in figure 3. Since the wire could not be calibrated, the actual value of the speed could not be obtained; but, with the wire carried at a constant temperature of about 110° C. above room temperature, the change in the voltage drop, as the wire was moved from one position to another, served to indicate changes in speed and hence in τ_0. The lower curve of figure 15 was obtained in this way. Although the minimum in the voltage curve is not sharp, it is possible to locate its position to within ± 0.05 in x/D. The position was estimated to be 1.13, or 4.5 inches from the leading edge.

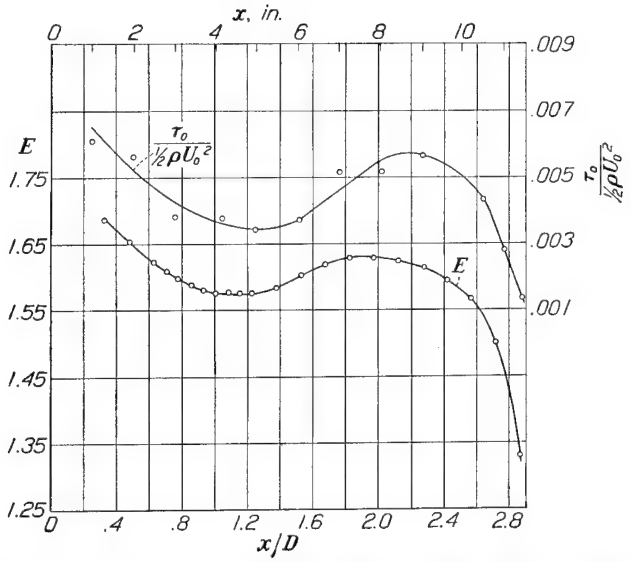

FIGURE 15.—Variation of shearing stress along surface of elliptic cylinder. τ_0, shearing stress at surface, computed from data of figures 11 and 12. E-curve obtained from hot wire on sliding band 0.008 inch from surface. E=voltage drop across wire.

The speed changes may be deduced roughly from the crossing of the contours by referring again to figure 12 and remembering that moving the wire by the sliding band at a height of 0.008 inch from the surface would correspond to passing along the abscissas of figure 12 at a height of $y/D=0.002$. It will be noted that the speed decreases to about $x/D=1.25$ and increases again beyond this point. Considering the coarseness of the diagram, this result is in satisfactory agreement with figure 15, which places the minimum at $x/D=1.13$. The presence of transition is not greatly in evidence in figure 12 before 1.4, hence the minimum in the voltage curve of figure 15 possibly coincides with the very beginning of transition.

A somewhat different method of locating transition, involving the use of small pitot tubes, was employed by Jones (reference 13) in his study of transition on a wing in flight. The method depended on the change occurring in the mean speed distribution in the layer through the transition region. In order to detect the change, several small pitot tubes, arranged in a compact group, were placed within the layer at different distances from the surface and moved from one position to another. Jones points out that one pitot tube placed in contact with the surface is sufficient and may be used in wind-tunnel experiments but that in flight the bank of several tubes had certain advantages. A single pitot tube at the surface is nearly equivalent to the hot wire as used in the present experiment.

SPEED FLUCTUATIONS IN THE BOUNDARY LAYER

The point at $x/D=1.13$ ($x=4.5$ inches) having been identified as the point at which transition probably began, oscillograph records of the u-fluctuations in the layer were taken in the neighborhood of the 4.5-inch position, to detect a change in frequency. The records are shown in figure 16, the apparatus being the same as that used to obtain figure 8. It is not evident from mere inspection that any change in the average frequency has occurred in crossing the 4.5-inch position.

In view of the importance of finding additional evidence of transition, it seemed worth while to measure the distribution of the root-mean-square value of the u-fluctuations across the layer at a number of positions about the surface. Eleven distributions were determined at the same positions in which the mean-speed measurements with the higher turbulences were made. The hot-wire anemometer and the amplifier have been described in an earlier section. The length of the hot wire in the present case was 0.152 inch. Seven of the distributions are shown in figure 17. By comparison with the measurements given by Dryden in reference 3, the curves up to and including the one at 1.26 show a marked similarity to the laminar type, while those at 1.52, 1.76, and particularly the one at 2.88 show similarity to the turbulent type. It will be observed that the peaks of successive curves increase to a maximum and then decrease as the distribution changes over into the turbulent type. The decrease in the peak appears to begin between 1.00 and 1.26.

The contour diagram of figure 18 was prepared by taking values of y/D for particular values of u'/U_0 from faired curves, of which those shown in figure 17 are examples. On each curve of equal u'/U_0 the value is given, expressed as a percentage ($100\ u'/U_0$). This

diagram presents a picture of the fluctuations in the layer as a whole and again shows the region of large fluctuations near the surface in the neighborhood of $x/D=1.00$.

It will be recalled that the minimum in the skin friction, as indicated by the voltage curve of figure 15, fell at $x/D=1.13$, just midway between the curves at 1.00 and 1.26 in figure 17 where the peak in u'/U_0 began to decrease. It is also quite evident from figure 18 that the fluctuations possess certain singularities in this region. The evidence from the magnitude and the distribution of the fluctuations supports the assumption that the minimum in the skin friction denotes the beginning of transition. The fact that no frequency change was apparent in this region may be construed to mean that frequency change is an insensitive test of the beginning of a very gradual transition.

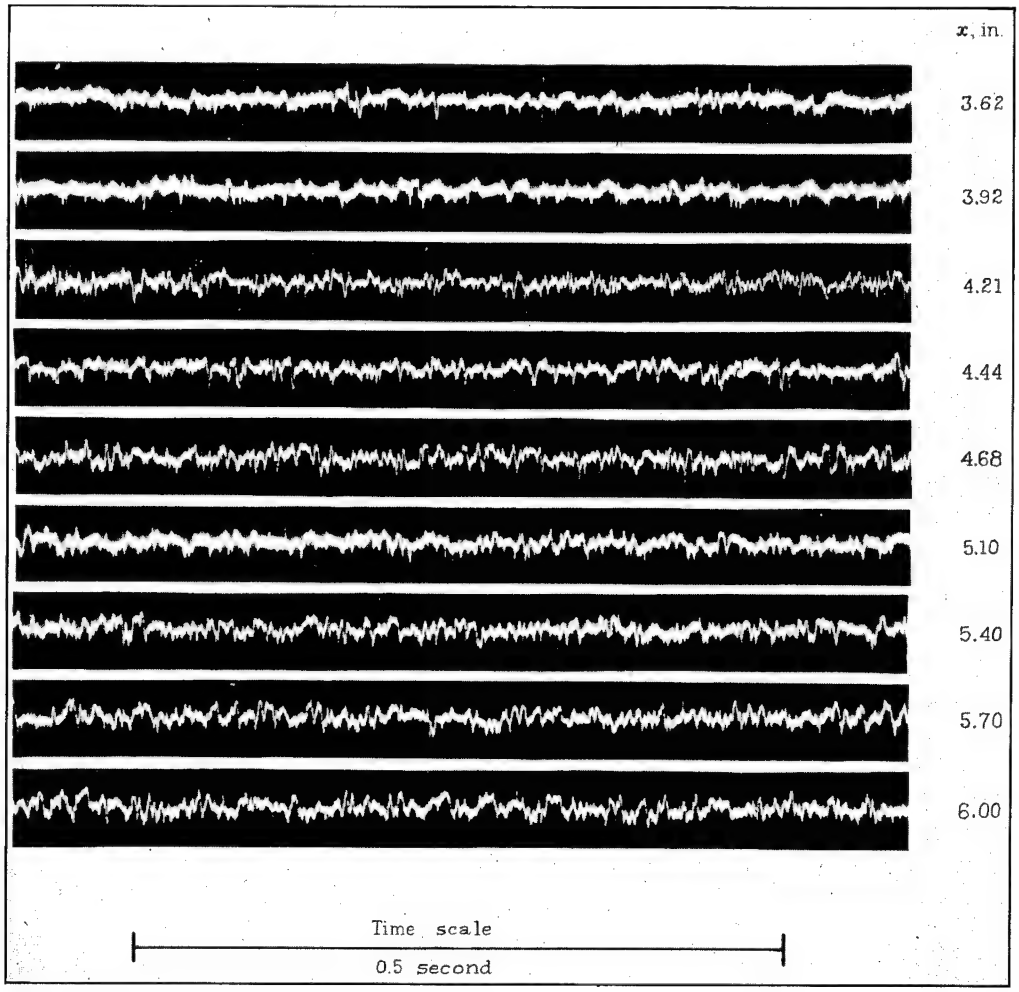

FIGURE 16.—Oscillograph records of u-fluctuations in boundary layer at 0.0158 inch from surface obtained with hot wire on sliding band. Air speed (U_0), 60 feet per second; stream turbulence as shown in figure 9.

EFFECT OF INTENSITY AND SCALE OF STREAM TURBULENCE ON TRANSITION

By the time the work already described had been done, it seemed fairly certain that a hot wire attached to a sliding band was a reliable device for indicating the beginning of transition. Since the simplicity of the procedure made it possible to detect transition very quickly, a somewhat extended investigation was undertaken to determine how the beginning point of transition shifted when the stream turbulence was changed. Several screens for producing turbulence were available, as part of the standard wind-tunnel equipment, for which the intensity and the scale of the turbulence were known as a function of distance downstream from the screen. The procedure was to vary the intensity of the turbulence, and to a limited extent the scale, by placing one of the screens at different distances upstream from the cylinder. The chief changes in scale were accomplished by using screens of different mesh size. The screens are described in table I. Measured values of intensity, u'/U_0, and scale, L, of the turbulence produced by these screens are given in reference 7. The values of u'/U_0 and L used in the present work were taken from the least-square lines of figures 10 and 7, respectively, of reference 7.

The variation of u'/U_0 and L with distance from the 1-inch screen is shown in figure 9. The figure illustrates one source of uncertainty in this procedure, namely, that u'/U_0 decreases from the leading to the trailing edge of the cylinder and L increases slightly, leaving the choice of values for u'/U_0 and L somewhat arbitrary. The change was the greater the smaller the mesh of the screens, hence screens of smaller mesh than the 1-inch were not used. There were available, besides the 1-inch mesh, a 3¼-inch and a 5-inch mesh, all screens being approximately geometrically similar.

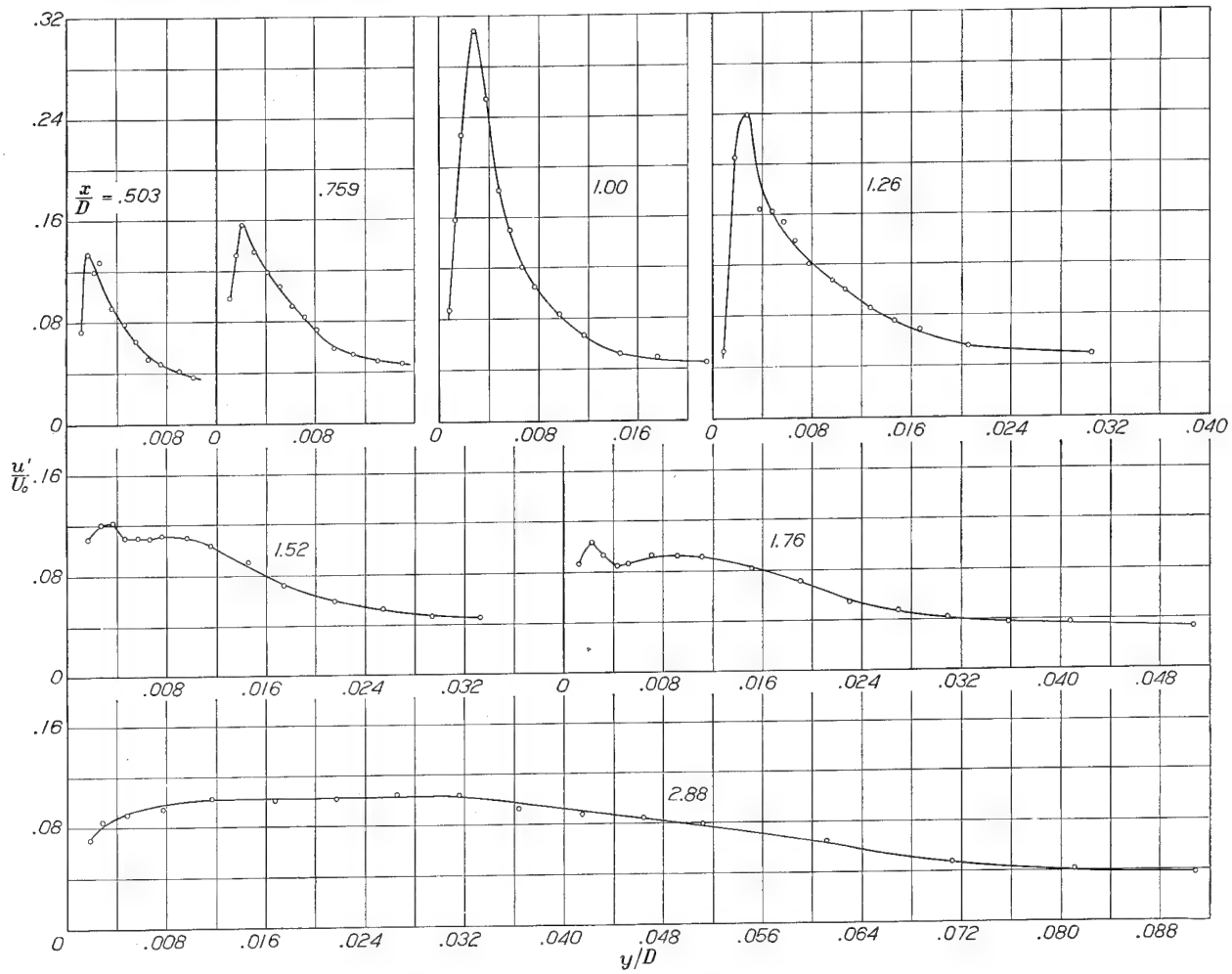

FIGURE 17.—Distribution of u-fluctuations in boundary layer. Air speed (U_0), 60 feet per second; stream turbulence as shown in figure 9.

In order to specify a definite value of intensity and scale, the values of u'/U_0 and L selected were those found in the undisturbed stream at the section of the tunnel midway between the leading edge of the cylinder and the beginning of transition.

In order to avoid irregularities in the average speed over the cross section of the stream and to insure isotropic turbulence, the screens were not placed nearer to the leading edge than 16 mesh lengths. In the investigation reported in reference 7, it was found that the regular pattern of maxima and minima in mean speed caused by the wake of the individual wires disappeared at distances of about 12 mesh lengths for all the screens. The uniformity of speed back of the screens is treated in detail in reference 7.

The sliding band and the mechanism for moving it have already been described in connection with figure 3. A wire 0.00063 inch in diameter and 0.5 inch long was attached to the band at a distance of 0.008 inch from the surface, the set-up being the same as that used to obtain the voltage curve of figure 15. The wire was connected as one arm of a Wheatstone bridge, which was used in the preliminary part of the work to hold the wire at a fixed temperature of about 100° C. above room temperature while the voltage across the wire was read on a potentiometer. Later the procedure was changed simply to reading the unbalance of the bridge on a galvanometer for each position of the band. Since the two methods gave curves with minima in identical positions, the latter method was adopted because of the rapidity with which readings could be taken.

Figure 19 gives three examples of the type of curve obtained when the galvanometer reading was plotted against position of the wire. The wind speed was set

at 60 feet per second in each case, giving a fixed Reynolds Number of 118,000, and the turbulence was varied by shifting the position of the 1-inch screen. Curve A was obtained with the screen 18 inches ahead of the leading edge of the cylinder, curve B with the screen 24 inches ahead, and curve C with the screen 33 inches ahead. Since the same screen was used, the shift in the position of the minimum along the abscissa is due mainly to the change in the intensity of the turbulence.

The minimum was usually found from a more complete curve like those shown in figure 15; then, with the galvanometer sensitivity greatly increased, the region of the minimum was explored in detail, as in figure 19. An unaccounted-for irregularity in the curves was always found near the 4-inch position. The irregularity was small compared with the minimum denoting transition and was never confused with it but, when the two fell close together, the irregularity in the curve tended to obscure the position of the minimum.

A somewhat puzzling situation was encountered when curves were obtained with no screen in the tunnel and the lowest condition of turbulence prevailed. It will be recalled that all available evidence pointed to a laminar separation under this condition with the turbulent layer developing only after separation. It was surprising, therefore, to find the curves shown in figure 20 with an

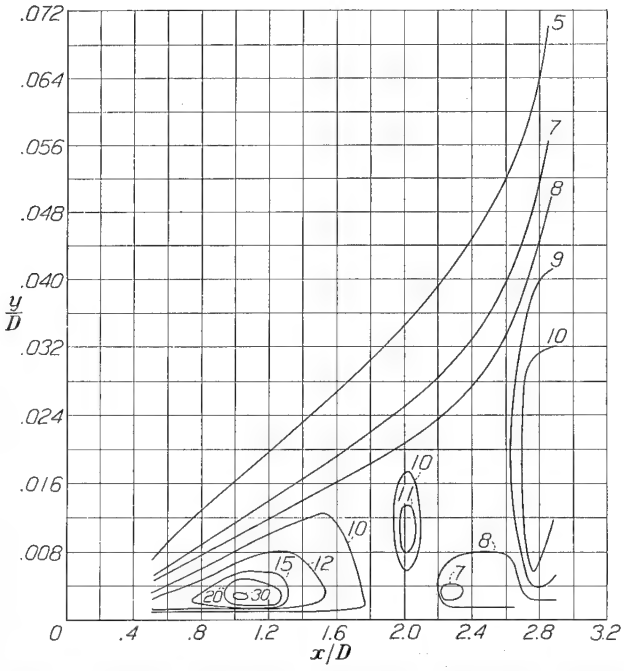

FIGURE 18.—Contours of equal u'/U_0 in boundary layer. Numbers on curves give values of 100 u'/U_0. Air speed, 60 feet per second; stream turbulence as show in figure 9.

unmistakable minimum near the 6.1-inch position, much ahead of separation at the 10-inch position. Curves taken at successively decreasing speeds showed minima gradually fading into an inflection and then disappearing. The minima in figure 20 back of the 8-inch position are the result of separation, the ensuing rise following the minima being caused either by a reattachment of the layer or reverse flow. It should be pointed out that, even though a minimum is found in the separation region, the hot wire and the sliding band is not an appro-

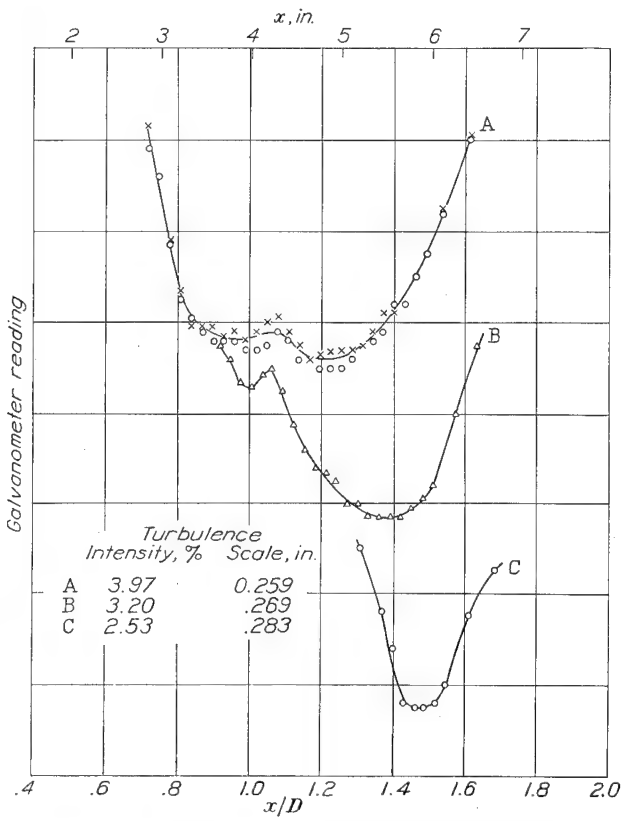

FIGURE 19.—Effect of stream turbulence on position of skin friction minima. Turbulence produced by 1-inch screen. Air speed (U_0), 60 feet per second; hot wire on sliding band 0.008 inch from surface.

priate device for accurately locating separation because of the insensitivity of the wire to direction of flow. In general, the minima do not coincide exactly with the position of separation as indicated by kerosene and lampblack.

Another feature of the minima shown in figure 20 is that they do not shift appreciably from the 6.1-inch position as the speed of the stream is changed. It was noted also, when the speed was kept constant at 60 feet per second and the turbulence was varied by screens, that the intensity could be raised to about 2 percent with the 1-inch screen and still higher with the larger screens before the minimum moved perceptibly from the 6.1-inch position. These facts made the connection between the minima at this point and transition look somewhat doubtful. If the minima were really due to the beginning of transition, the boundary layer just back of the 6.1-inch position was evidently unstable enough to permit transition at all but very low speeds and was so stable just ahead of this position that only high speed and high intensity of turbulence could cause transition to progress forward. To account for such a

condition one is led to look for some natural cause of instability at this point.

It is known that pressure gradient has a marked influence on transition, an accelerating pressure gradient tending to prevent transition and an opposing pressure gradient tending to promote transition. Figures 4 and

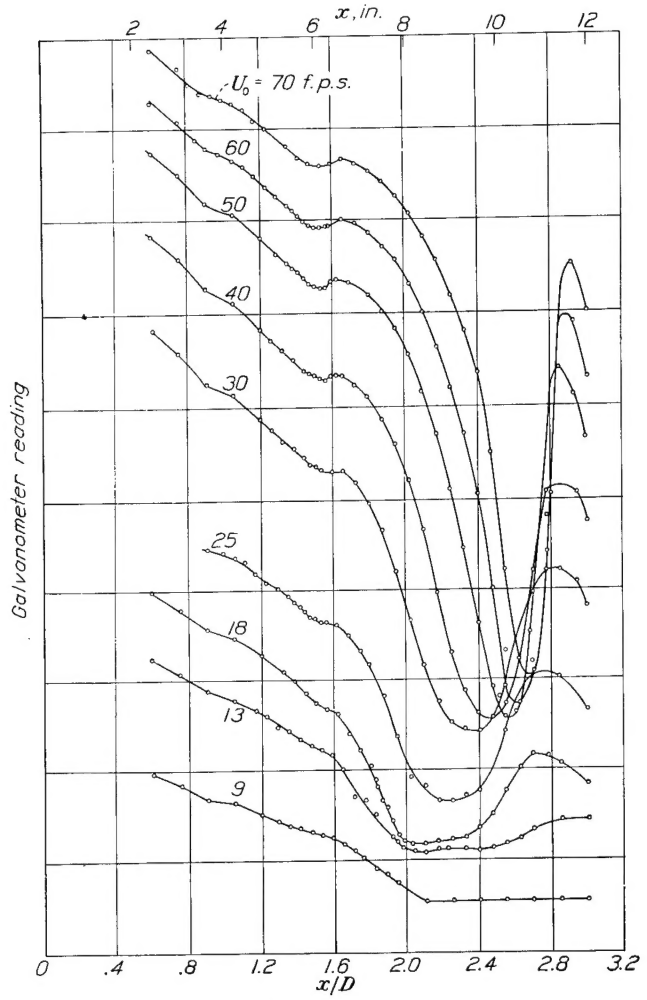

FIGURE 20.—Skin friction minima in boundary layer of elliptic cylinder for free tunnel condition; stream turbulence, 0.85 percent.

10 show that the 6.1-inch position roughly divides the accelerating from the opposing pressure gradient at the lower speeds and, at the higher speeds, marks the end of the accelerating pressure gradient. The 6.1-inch position appears therefore to be the first favorable one for transition.

The possibility that transition might remain relatively fixed in this position until the speed and the turbulence became sufficiently high may be seen in the following way. At the lower speeds, the presence of an opposing pressure gradient makes transition easy. As the speed is raised, the increasing boundary-layer Reynolds Number tends to move transition forward, but this effect is counteracted at first by a decrease in the opposing pressure gradient accompanying the increased speed and later by a slight increase in the accelerating pressure gradient. It is well known that transition rarely occurs in a region of accelerating pressure gradient, hence the necessity for high turbulence to force transition ahead of 6.1 inches. The beginning of transition coinciding with a minimum in the 6.1-inch position is therefore not contradictory to reason. When such behavior of the minimum as movement forward with sufficiently increased turbulence and disappearance with sufficiently increased speed was considered in addition, it was impossible to escape the conclusion that this minimum was not like the fixed irregularity at the 4-inch position but was associated with the beginning of transition just as definitely as the minima in figure 15.

Curves similar to those of figure 19 were next obtained with the 3¼- and 5-inch screens, the speed in all cases being 60 feet per second. The positions of the minima, found from the several curves, were then plotted against the intensity of the turbulence from the different screens to give the three curves shown in figure 21. The effect of the scale is quite evident from the separation of the curves. Figure 21 shows that a greater intensity of large-scale turbulence is required to move transition forward than is required of a turbulence of

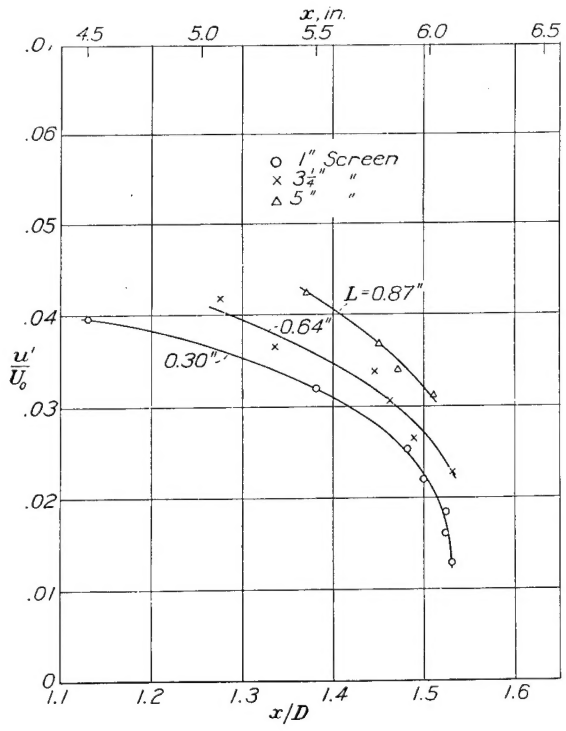

FIGURE 21.—Effect of stream turbulence on position of transition, showing effect of intensity and scale. Air speed, 60 feet per second; R, 118,000.

small scale. The turbulence is therefore the more effective the smaller the scale.

In reference 7 a similar effect is shown for spheres, where, for a given intensity, a small-scale turbulence lowered the critical Reynolds Number of spheres more than did a large-scale turbulence. In reference 14, G. I. Taylor has suggested a functional relation between

the critical Reynolds Number of spheres and the scale and intensity of the turbulence. His relation is

$$R_c = f\left[\frac{u'}{U_0}\left(\frac{D}{L}\right)^{1/5}\right]$$

where R_c is the critical Reynolds Number, D is the diameter of the sphere, and f is a function to be determined by experiment. In figure 18 of reference 7, this relation was tested by plotting $\frac{u'}{U_0}\left(\frac{D}{L}\right)^{1/5}$ against R_c. The results for a 5-inch and an 8.55-inch sphere and for turbulence ranging in scale from 1.25 inches to 0.055 inch approximate a single curve to within the observational error.

The details of the development of Taylor's relation are discussed in reference 14. It may be stated in general terms that the foregoing combination of intensity and scale occurs in the expression for the root-mean-square pressure gradient in the turbulent flow and that the effect of turbulence is assumed to be that of the pressure gradient on transition. The critical Reynolds Number was brought into the relation by assuming that the critical Reynolds Number corresponded to a definite position of transition on the sphere for all conditions of turbulence. With the position of transition fixed, the critical Reynolds Number became the variable.

In the case of the elliptic cylinder the procedure was arranged so that the Reynolds Number remained fixed and the position of transition was allowed to vary. There should therefore exist a functional relation between position of transition and the same combination of scale and intensity of the turbulence.

In figure 22, $\frac{u'}{U_0}\left(\frac{D}{L}\right)^{1/5}$ has been plotted against the observed position of the minima. For each point the value of u'/U_0 and L was taken as that corresponding to the undisturbed stream at the section of the tunnel midway between the leading edge of the cylinder and the position of the point on the surface. This procedure for selecting u'/U_0 and L was adopted on the assumption that no one part of the laminar layer was more sensitive to outside disturbances than another. It will be observed that the points fall nearer to a single curve in this figure than they do in figure 21, where the scale was not taken into account. Although there are systematic departures from the curve of figure 22, these departures do not follow in the order of the changes in scale, i. e., the points for the 3¼-inch screen tend to lie below the curve, whereas those for the 5-inch screen tend to lie above the curve. In this connection, it should be pointed out that the sliding-band method was not entirely free from systematic errors, for it was found that the position of the minimum became displaced slightly if at any time the band did not fit the cylinder snugly. The magnitude of the shift was large enough to cause the systematic differences in figure 22.

This part of the investigation has dealt with only the beginning of transition. It seems entirely possible that turbulence may affect the extent of transition as well as the beginning, in which case the full effect of turbulence is not taken into account. In consideration of this fact, together with the uncertainties inherent in the procedure and the arbitrariness in the choice of u'/U_0 and L, the approximation to a single curve in figure 22 is as good as may be expected. Taylor's theory therefore appears to account for the relative effects of the scale and the intensity of stream turbulence on transition to as close a degree of approximation as the present experiment can detect.

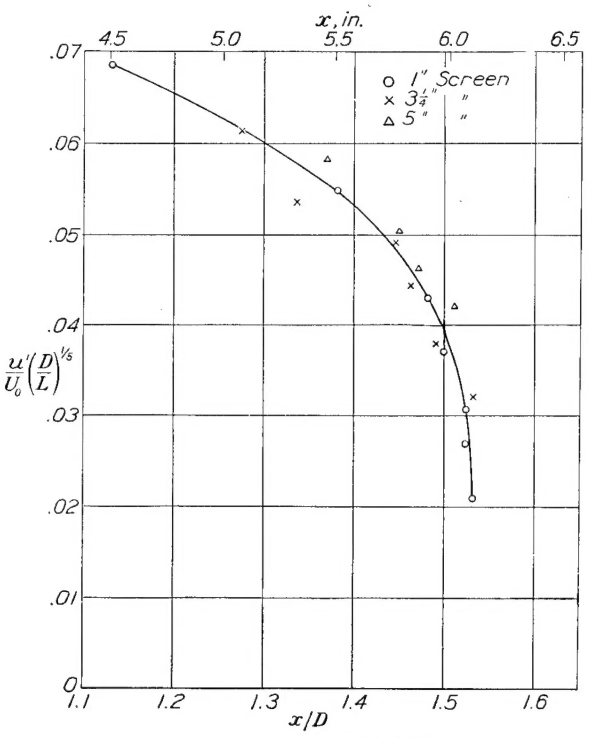

FIGURE 22.—Position of transition as function of $\frac{u'}{U_0}\left(\frac{D}{L}\right)^{1/5}$. Air speed, 60 feet per second; R, 118,000.

CONCLUSION

A case has been presented in which boundary-layer separation was followed by a reattachment of the layer to the surface. Transition occurred in the separation zone and the reattached layer was turbulent. The separation was of a nearly laminar type but not purely laminar because of a very incomplete transition beginning ahead of the separation point near the pressure minimum. This case might be called "transition by separation," although such a designation would not mark the phenomenon as unique, since transition probably always occurs somewhere in the detached layer after a laminar or nearly laminar separation. It was probably the occurrence of this transition near the separation point, brought about by a particular set of conditions, that made a reattachment of the layer

possible. The conditions were a low stream turbulence and a Reynolds Number in the neighborhood of 139,000.

When the stream turbulence was raised to about 4 percent, it was impossible to obtain separation before transition at any Reynolds Number. In this case, transition took place gradually, beginning at 4½ inches from the leading edge of the elliptic cylinder.

It was shown that the minimum in the distribution of skin friction along the surface of the cylinder marked the beginning of transition and that a hot wire mounted on a sliding band served as a satisfactory device for finding the minimum.

At a fixed Reynolds Number, the position of the beginning of transition on the cylinder was found to depend on the scale of the turbulence as well as on the intensity. A functional relation was found to exist between the position x/D of the beginning of transition and $\frac{u'}{U_0}\left(\frac{D}{L}\right)^{1/5}$.

NATIONAL BUREAU OF STANDARDS,
Washington, D. C., August 6, 1938.

TABLE I.—DIMENSIONS OF SQUARE-MESH SCREENS FOR PRODUCING TURBULENCE

Nominal mesh, in.	Average measured mesh, in.	Average measured wire or rod diameter, in.	Material
1	1.007	0.196	Iron wire.
3¼	3.285	.626	Cylindrical wooden rods.
5	5.016	.976	Cylindrical wooden rods.

REFERENCES

1. Schubauer, G. B.: Air Flow in a Separating Laminar Boundary Layer. T. R. No. 527, N. A. C. A., 1935.
2. King, L. V.: On the Convection of Heat from Small Cylinders in a Stream of Fluid: Determination of the Convection Constants of Small Platinum Wires with Applications to Hot-Wire Anemometry. Phil. Trans Roy. Soc., vol. 214, 1914, pp. 373–432.
3. Dryden, Hugh L.: Air Flow in the Boundary Layer Near a Plate. T. R. No. 562, N. A. C. A., 1936.
4. Mock, W. C., Jr.: Alternating-Current Equipment for the Measurement of Fluctuations of Air Speed in Turbulent Flow. T. R. No. 598, N. A. C. A., 1937.
5. Dryden, H. L., and Kuethe, A. M.: Effect of Turbulence in Wind Tunnel Measurements. T. R. No. 342, N. A. C. A., 1930.
6. Dryden, H. L., and Kuethe, A. M.: The Measurement of Fluctuations of Air Speed by the Hot-Wire Anemometer. T. R. No. 320, N. A. C. A., 1929.
7. Dryden, Hugh L., Schubauer, G. B., Mock, W. C., Jr., and Skramstad, H. K.: Measurements of Intensity and Scale of Wind-Tunnel Turbulence and Their Relation to the Critical Reynolds Number of Spheres. T. R. No. 581, N. A. C. A., 1937.
8. Fediaevsky, K.: Turbulent Boundary Layer of an Airfoil. T. M. No. 822, N. A. C. A., 1937.
9. Pohlhausen, K.: Zur näherungsweisen Integration der Differentialgleichung der laminaren Grenzschicht. Z. f. a. M. M., Bd. 1, 1921, S. 252–268.
10. von Kármán, Th., and Millikan, C. B.: On the Theory of Laminar Boundary Layers Involving Separation. T. R. No. 504, N. A. C. A., 1934.
11. von Doenhoff, Albert E.: An Application of the von Kármán-Millikan Laminar Boundary-Layer Theory and Comparison with Experiment. T. N. No. 544, N. A. C. A., 1935.
12. Fage, A.: Experiments on a Sphere at Critical Reynolds Numbers. R. & M. No. 1766, British A. R. C., 1937.
13. Jones, B. Melvill: Flight Experiments on the Boundary Layer. Jour. Aero. Sci., vol. 5, no. 3, Jan. 1938, pp. 81–94.
14. Taylor, G. I.: Statistical Theory of Turbulence. V. Effect of Turbulence on Boundary Layer. Theoretical Discussion of Relationship between Scale of Turbulence and Critical Resistance of Spheres. Proc. Roy. Soc. (London), ser. A, vol. 156, no. 888, Aug. 1936, pp. 307–317

U. S. GOVERNMENT PRINTING OFFICE: 1939

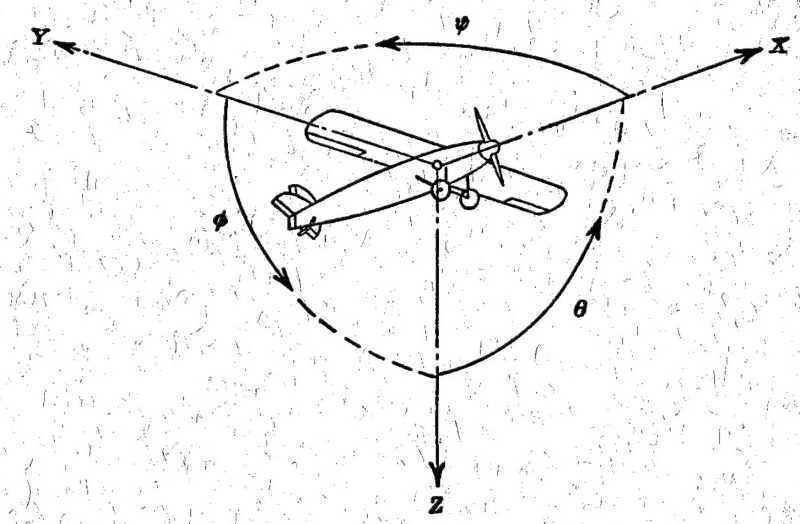

Positive directions of axes and angles (forces and moments) are shown by arrows

Axis		Force (parallel to axis) symbol	Moment about axis			Angle		Velocities	
Designation	Symbol		Designation	Symbol	Positive direction	Designation	Symbol	Linear (component along axis)	Angular
Longitudinal	X	X	Rolling	L	$Y \longrightarrow Z$	Roll	ϕ	u	p
Lateral	Y	Y	Pitching	M	$Z \longrightarrow X$	Pitch	θ	v	q
Normal	Z	Z	Yawing	N	$X \longrightarrow Y$	Yaw	ψ	w	r

Absolute coefficients of moment

$C_l = \frac{L}{qbS}$ (rolling) $\quad C_m = \frac{M}{qcS}$ (pitching) $\quad C_n = \frac{N}{qbS}$ (yawing)

Angle of set of control surface (relative to neutral position), δ. (Indicate surface by proper subscript.)

4. PROPELLER SYMBOLS

D, Diameter

p, Geometric pitch

p/D, Pitch ratio

V', Inflow velocity

V_s, Slipstream velocity

T, Thrust, absolute coefficient $C_T = \frac{T}{\rho n^2 D^4}$

Q, Torque, absolute coefficient $C_Q = \frac{Q}{\rho n^2 D^5}$

P, Power, absolute coefficient $C_P = \frac{P}{\rho n^3 D^5}$

C_s, Speed-power coefficient $= \sqrt[5]{\frac{\rho V^5}{P n^2}}$

η, Efficiency

n, Revolutions per second, r.p.s.

Φ, Effective helix angle $= \tan^{-1}\left(\frac{V}{2\pi r n}\right)$

5. NUMERICAL RELATIONS

1 hp.=76.04 kg-m/s=550 ft-lb./sec.
1 metric horsepower=1.0132 hp.
1 m.p.h.=0.4470 m.p.s.
1 m.p.s.=2.2369 m.p.h.

1 lb.=0.4536 kg.
1 kg=2.2046 lb.
1 mi.=1,609.35 m=5,280 ft.
1 m=3.2808 ft.